List of changes in manuscript

August 12, 2015

We are very thankful to the reviewers for their insightful evaluation of our work. Their comments and questions have led to various corrections and improvements of the manuscript. Please find below a list of the main revisions that we have made following the reviewers' suggestions. Revisions are marked by the blue text in the attached revised manuscript.

- New figures 1, 2, 5a and 6a are added.
- Errors in equations are corrected.
- We now use a threshold value of $J_\varepsilon = 10^9\,\mathrm{L}^{-1}\,\mathrm{s}^{-1}$, and a deposition coefficient $\alpha = 0.1$ for the reference case. All calculation has been revised using these new values. Please note that our conclusions do not change qualitatively.
- The bibliography has been improved, with the addition of the following references: Hermann et al. (2003); Barahona and Nenes (2011); Murphy (2014); Shi et al. (2015).

References

Barahona, D. and Nenes, A.: Dynamical states of low temperature cirrus, Atmos. Chem. Phys., 11, 3757–3771, doi:10.5194/acp-11-3757-2011, 2011.

Hermann, M., Zahn, A., Heinrich, G., and Brenninkmeijer, C. A. M.: Meridional distributions of aerosol particle number concentrations in the upper troposphere and lower stratosphere obtained by Civil Aircraft for Regular Investigation of the Atmosphere Based on an Instrument Container (CARIBIC) flights, J. Geophys. Res., 108, D3, doi: 10.1029/2001JD001077, 2003.

Murphy, D. M.: Rare temperature histories and cirrus ice number density in a parcel and one-dimensional model, Atmos. Chem. Phys. Discuss., 14, 10 701–10 723, doi: 10.5194/acpd-14-10701-2014, 2014.

Shi, X., Liu, X., and Zhang, K.: Effects of preexisting ice crystals on cirrus clouds and comparison between different ice nucleation parameterizations with the Community Atmosphere Model (CAM5), Atmos. Chem. Phys., 15, 1503–1520, doi:10.5194/acp-15-1503-2015, 2015.

Effect of gravity wave temperature fluctuations on homogeneous ice nucleation in the tropical tropopause layer

June 10, 2015

We would like to thank the reviewer for the insightful evaluation of our work, which will guide us to revise and improve the manuscript. Please find below our point-by-point reply.

1. ***Reviewer*** — Measurements of ice crystal number concentrations in the TTL cirrus usually yield values that are substantially lower than a theory based on the assumption of homogeneous nucleation would predict. This so called "ice nucleation puzzle" (Spichtinger and Krämer, 2013) can be solved by assuming temperature fluctuations (caused by fluctuations of the vertical wind) with time scales similar to the nucleation time scale (e.g. triggered by gravity waves). So far, simulations using idealistic temperature time series have been used to demonstrate this. The present authors want to go a step further and use measured time series of temperature. I endorse this goal.

   The balloon measurements from which the time series are obtained, must be filtered at the high frequency (short period) end, at a period of 10 min. That is, processes that are faster, cannot be treated with this method. Unfortunately, homogeneous nucleation is such a quick process and to my opinion the authors miss their goal. It seems, however, that the authors found a trick to circumvent this problem, namely to choose an extremely low nucleation threshold. This trick works insofar as it extends the nucleation time scales to a few minutes up to an hour (Sect. 4.3.1). However, this is achieved only for a high price. Usually the threshold is chosen in a way that the nucleation rate is practically zero below the threshold and many orders of magnitude larger above it. In this paper the nucleation rate at the threshold and some percent above is practically zero as well (see Fig. 3). It seems that this makes results differing from corresponding results from other papers, qualitatively and quantitatively. This choice of threshold and the consequent differences from results from other papers are not discussed at all; instead the authors claim consistency with other results, a view that I cannot support.

   My recommendation is therefore to accept the paper only after a major revision (addition) where the authors demonstrate either that their nucleation results are similar and consistent with those of other authors (e.g. Kärcher and Lohmann, 2002; Spichtinger and Gierens, 2009) or that those other results are wrong. This is a pity, because the paper does contain an interesting concept, i.e. the distinction between vapour- and temperature-limit nucleation events. I like also the analytical derivation in Sect. 5.

Authors — Our cut-off frequency choice is driven by the search of a compromise between incorporating the gravity wave disturbances as thoroughly as possible while avoiding motions associated with the balloon flight mechanics. In particular, the balloon neutral oscillations have periods $\sim 4\,\mathrm{min}$, and that is why we used a safe ($f_{\mathrm{high}} = (10\,\mathrm{min})^{-1} = 0.1\,\mathrm{min}^{-1}$) cut-off frequency. As stated in the manuscript, the chosen cut-off frequency enables us to virtually resolve the whole spectrum of gravity-waves in most of the TTL. Higher frequency motions are typically associated with turbulence past the Brunt-Väisälä frequency. Nevertheless, we compare here the microphysical simulations with filtered data at cut-off frequencies of $0.2\,\mathrm{min}^{-1}$, and $0.1\,\mathrm{min}^{-1}$ (original value). For the data set with $f_{\mathrm{high}} = 0.2\,\mathrm{min}^{-1}$, we additionally apply a butterworth filter to eliminate the residual balloon-induced motions (see Fig. 1 below). Figure 2 shows that the number of ice crystals as a function of $\triangle S$ (or $\triangle T$) is not sensitive to the cut-off frequency.

The nucleation threshold is a parameter associated with the numerics that allows us to precisely define the beginning and end of the nucleation events. The reviewer is concerned that the threshold that we chose for our simulations was too small. To address this, we are now using a threshold of $J_\epsilon = 10^9\,\mathrm{L}^{-1}\,\mathrm{s}^{-1}$, compared with the original value of $1\,\mathrm{L}^{-1}\,\mathrm{s}^{-1}$. In general, the duration of nucleation is shorter with larger J_ϵ (compare Fig. 3 here with Fig. 4 in the manuscript). However, the specific choice of the threshold does not usually affect the total number of ice crystals N_{i}. This is because N_{i} depends largely on the maximum nucleation rate J_{max} (and not on J_ϵ), as long as $J_{\mathrm{max}} \gg J_\epsilon$.

In summary, the statistics of N_{i} as a function of $\triangle S$ (or $\triangle T$) is independent of the parameters f_{high} and J_ϵ. Our conclusions are based on this statistics, and are confirmed by the analytical derivation in Sect. 5.1 of the manuscript. Please note that the mathematics in this section applies regardless of the chosen threshold of nucleation as well as the nature of the waves in the temperature time series.

As pointed out by the reviewer, the INCs shown in Fig. 2 of the manuscript are indeed larger than in other papers, specifically Kärcher and Lohmann (2002, Fig. 3), and Spichtinger and Gierens (2009, Fig. 7). This difference is because we set the deposition coefficient to be $\alpha = 0.05$ for the calculation in this figure, while Kärcher and Lohmann (2002) used $\alpha = 0.5$. We are able to obtain consistent numbers as in these previous work with larger values of α (see Fig. 4). As mentioned in the manuscript, the deposition coefficient is poorly constrained by experimental data. The sensitivity of the INCs to the deposition coefficient ranging between 0.001 and 1 is discussed further in Sects. 4.3.3 and 5.2 of the manuscript.

2. ***Reviewer*** — Page 8777, line 20: I am surprised of the low critical saturation that you assume at 195 K. Looking at Fig. 3 of Koop et al. (2000) it seems that the critical supersaturation at 195 K is much higher. Using Eq. (4) from Kärcher and Lohmann (2002) I calculate $S_0 = 1.645$.

   Authors — The saturation ratio at the threshold of nucleation increases with the chosen threshold J_ϵ. We now have $S_0 = 1.553$ for $J_\epsilon = 10^9\,\mathrm{L}^{-1}\,\mathrm{s}^{-1}$. For an aerosol radius of $r_{\mathrm{a}} = 0.25\,\mu\mathrm{m}$ and aerosol number concentration of $N_{\mathrm{a}} = 200\,\mathrm{cm}^{-3}$, this corresponds to a production rate of $\frac{\mathrm{d}N}{\mathrm{d}t} = 0.013\,\mathrm{L}^{-1}\,\mathrm{s}^{-1}$ which is in the same order as that used in Spichtinger and Krämer (2013). Please note that Koop et al. (2000) plot the nucleation threshold S_0 for a freezing probability of $1\,\mathrm{min}^{-1}$, which corresponds to two-thirds of the

aerosol population being frozen in 1 min. They do not claim that their formula should only be applied above this threshold. To our understanding, the lower the threshold the more accurate the result.

Please also note that we have updated the formula for the water activity based on Koop and Zobrist (2009, Appendix), which is different from the original formula in Koop et al. (2000). In addition, we now use the formula for the saturation water vapour pressure given in Murphy and Koop (2005), instead of the Goff-Gratch formula used in the original manuscript. These updates also change the value of S_0 slightly.

3. ***Reviewer*** — Figure 2: It might be that the low critical supersaturation or your assumption of a monodisperse aerosol leads to a much higher sensitivity N_i vs. w. From Kärcher and Lohmann (2002) I assume that $N_\mathrm{i} \propto w^{3/2}$ in most cases. Figure 2 shows a relation that is rather $N_\mathrm{i} \propto w^{5/2}$ for low w. Also the number of ice crystals is much (factor 30 or so) larger in your model than for instance in Kärcher and Lohmann (2002) or Spichtinger and Gierens (2009, Fig. 7). These differences require an explanation.

   Authors — Please see the INCs as a function of w for the different values of the deposition coefficient in Fig. 4 below. For $\alpha = 0.5$ our calculation gives very similar numbers as in these previous work, as well as in Spichtinger and Krämer (2013, Fig. 2).

4. ***Reviewer*** — Figure 3: To my opinion we see here another strange result of the choice of an extremely low nucleation threshold. As the top right panel shows, we are above the nucleation threshold from t_0 on, but it needs 12–13 min before the curve in the bottom panel indicates an Ni of 0.001 per litre, and it takes still 10 and more minutes until all ice crystals are formed. The simulations suggest that ice formation occurs on a time scale of half an hour or so. Compare this to Spichtinger and Krämer (2013, Fig. 1) where a time scale of 140 s is indicated. How can you state that these results are consistent?

   Authors — We are now using a larger threshold and thus the duration of nucleation is shorter. As shown in Fig. 3, we also have nucleation events that last for only one or two minutes. Please note that the threshold does not affect the INCs obtained after the nucleation events, as explained above.

5. ***Reviewer*** — Page 8774, line 8–9: "whole equatorial area" sounds exaggerated considering that there are only 2 balloons.

   Authors — We agree and will rewrite this as "whole equatorial circle."

6. ***Reviewer*** — Eq. (1): R should be R_a.

   Authors — Thanks. We will fix this typo.

7. ***Reviewer*** — Section 3, par. 4: Please explain why sedimentation would reduce INC. If crystals get lost from the parcel by sedimentation, another nucleation event could occur earlier than without sedimentation. Why should this not happen?

   Authors — We meant that sedimentation reduces the INC strictly within each nucleation event. If nucleation occurs following ice sedimentation, then we will count this occurrence as a new event.

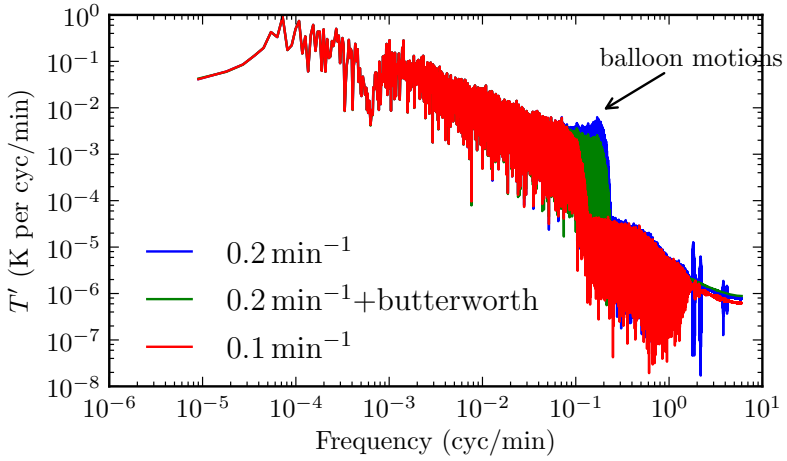

Figure 1: Power spectrum of the balloon temperature perturbations at cut-off frequencies of $0.2\,\mathrm{min}^{-1}$ and $0.1\,\mathrm{min}^{-1}$.

8. ***Reviewer*** — Beginning of Sect. 4: I do not understand how you can mention adiabatic motion and pressure variations in the first sentence, and assume constant air pressure in the second. Does "constant pressure" just mean that your parcels are sufficiently flat?

   Authors — The air parcels experience adiabatic motions, for which there are both pressure and temperature variations. However, the contribution associated with temperature variations to the variations in water vapour mixing ratio is much larger than that due to pressure variations. Thus, to calculate the water vapour mixing ratio of the air parcels we can assume constant pressure.

9. ***Reviewer*** — Figure 6 and Sect. 4.3.2: It is not easy to understand why $N_\mathrm{i}(210\,\mathrm{K})$ is higher than $N_\mathrm{i}(180\,\mathrm{K})$ as a function of $S_\mathrm{max} - S_0$ and vice versa as a function of $T_\mathrm{min} - T_0$. A more detailed explanation would be welcome.

   Authors — Indeed. We will add explanation to the revised manuscript. This comes from the dependence of a_w on T_0 (Eq. 18): a_w increases with increasing temperature, hence the different slopes of the functions $N_\mathrm{i}(S_\mathrm{max} - S_0)$ and $N_\mathrm{i}(T_\mathrm{min} - T_0)$ at different temperatures.

10. ***Reviewer*** — Eq. (19) and following text: if t^* is the point in time where $J = J_\mathrm{max}$ and $S = S_\mathrm{max}$, then $\mathrm{d}S/\mathrm{d}t$ should be zero.

    Authors — Yes, thank you for pointing this out. This eliminates the second term in Eq. (19).

References

Kärcher, B. and Lohmann, U.: A parameterization of cirrus cloud formation: Homogeneous freezing of supercooled aerosols, J. Geophys. Res., 107, D2, doi:10.1029/2001JD000470, 2002.

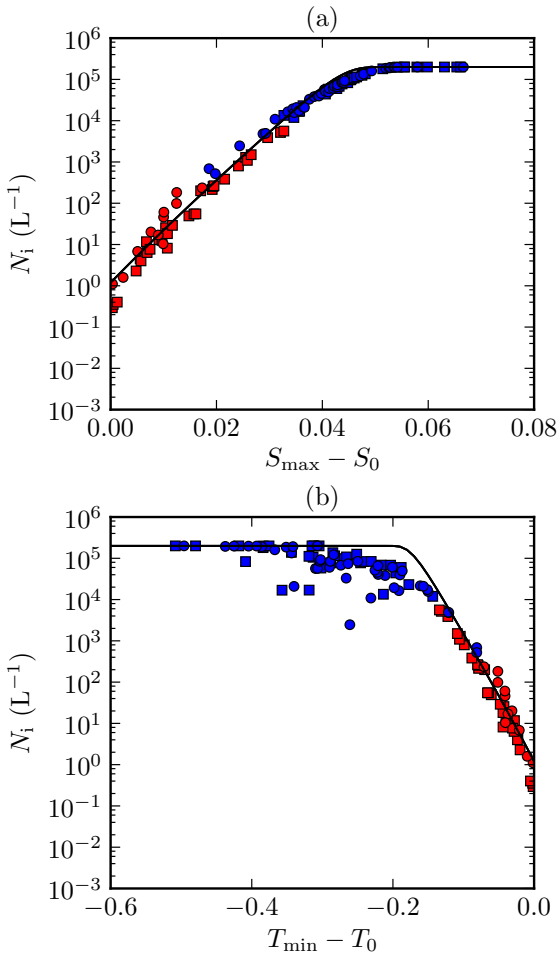

Figure 2: Number of ice crystals nucleated using the balloon temperature data, which has been filtered at high cut-off frequencies of $0.2\,\mathrm{min}^{-1}$ (squares) and $0.1\,\mathrm{min}^{-1}$ (circles). Blue markers show vapour-limit events and red markers show temperature-limit events. The threshold of nucleation is $J_\epsilon = 10^9\,\mathrm{L}^{-1}\,\mathrm{s}^{-1}$.

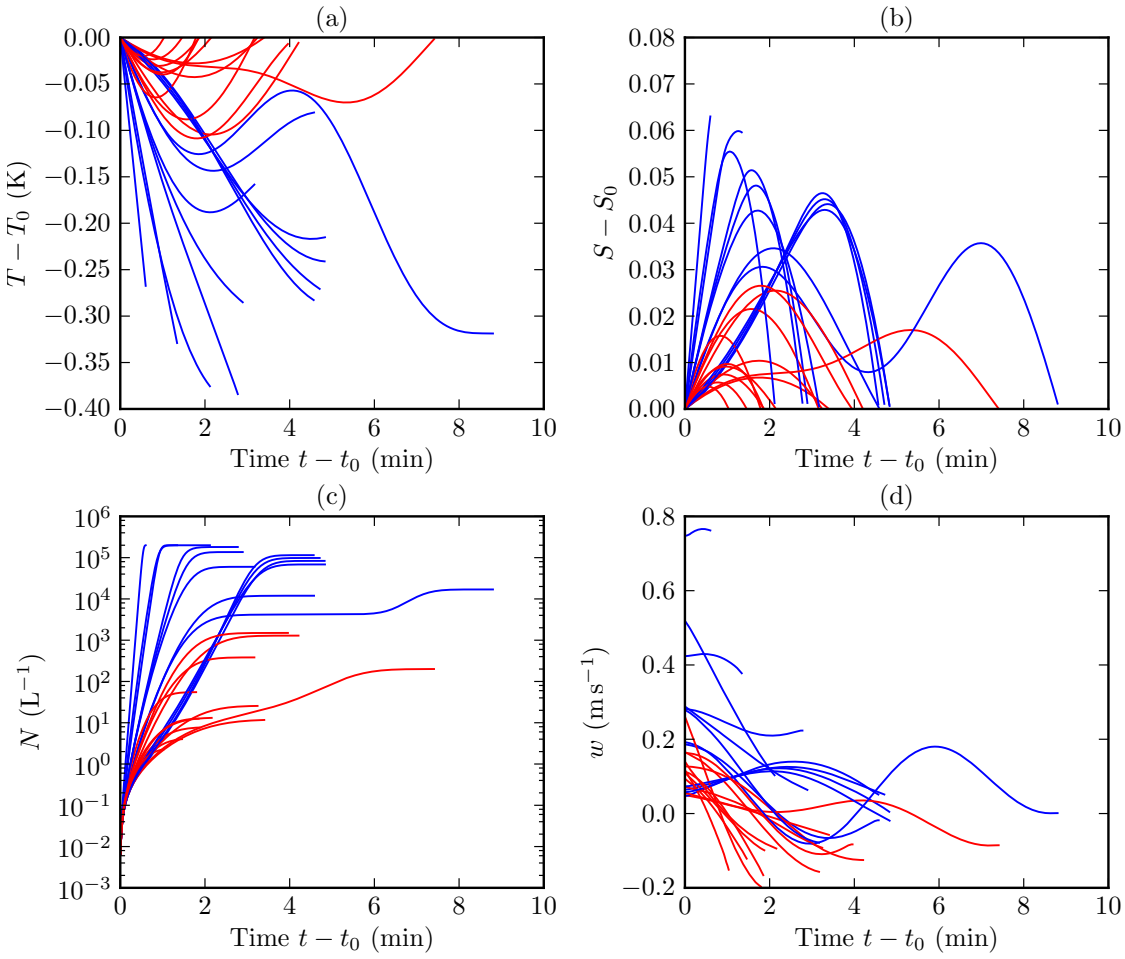

Figure 3: Evolution of temperature, saturation ratio, INC and vertical velocity during representative nucleation events forced by the balloon temperature data, which has been filtered at a high cut-off frequency of $0.2\,\mathrm{min}^{-1}$. Blue curves show vapour-limit events and red curves show temperature-limit events. The threshold of nucleation is $J_\epsilon = 10^9\,\mathrm{L}^{-1}\,\mathrm{s}^{-1}$.

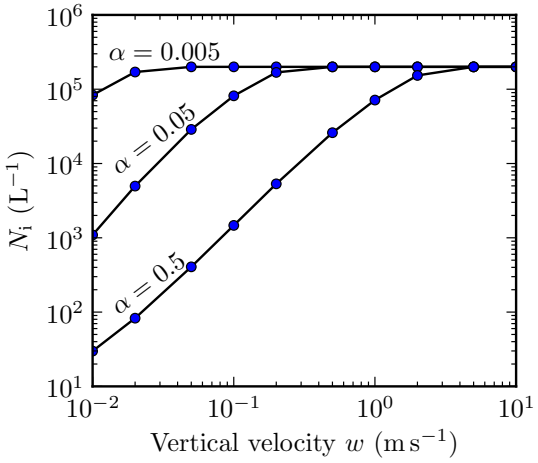

Figure 4: Number of ice crystals obtained for nucleation events forced by constant vertical velocity w for different values of the deposition coefficient α.

Koop, T. and Zobrist, B.: Parameterizations for ice nucleation in biological and atmospheric systems., Physical chemistry chemical physics : PCCP, 11, 10 839–10 850, doi: 10.1039/b914289d, 2009.

Koop, T., Luo, B., Tsias, A., and Peter, T.: Water activity as the determinant for homogeneous ice nucleation in aqueous solutions, Nature, 406, 611–614, doi:10.1038/35020537, 2000.

Murphy, D. M. and Koop, T.: Review of the vapour pressures of ice and supercooled water for atmospheric applications, Q. J. R. Meteorol. Soc., 131, 1539–1565, doi: 10.1256/qj.04.94, 2005.

Spichtinger, P. and Gierens, K. M.: Modelling of cirrus clouds - Part 1a: Model description and validation, Atmos. Chem. Phys., 9, 685–706, doi:10.5194/acp-9-685-2009, 2009.

Spichtinger, P. and Krämer, M.: Tropical tropopause ice clouds: a dynamic approach to the mystery of low crystal numbers, Atmos. Chem. Phys., 13, 9801–9818, doi:10.5194/acp-13-9801-2013, 2013.

Effect of gravity wave temperature fluctuations on homogeneous ice nucleation in the tropical tropopause layer

June 10, 2015

We would like to thank the reviewer for these critical comments; they will be very helpful for us in our revision of the manuscript. Please find below our point-by-point reply.

1. ***Reviewer*** — The authors carefully set up their simulations so that the vertical velocity changes sign at least once before substantial nucleation rates are reached. This is a clever way to show their expected result but begs the question of how realistic the setup actually is.

   Authors — There is a misunderstanding here regarding the setup of the simulations. The cases in Sect. 4.2 where we designed w to change signs are shown only for illustration purposes. For the simulations with the balloon data we did not impose any constraint on w: it may change sign before substantial nucleation rates are reached (temperature-limit event), or not (vapour-limit event), and we show results for both of these types of events in the manuscript.

2. ***Reviewer*** — As noted by another reviewer, if the filtering of the balloon measurements is applied differently, or if higher temperature fluctuations with periods below 10 min are allowed, the simulations may result in higher number concentration. In fact the authors claim that they can obtain small crystal number even for high vertical velocity, something that is never shown.

   Authors — We have addressed the question about the cut-off frequency used for filtering the data in our response to Reviewer 1. Our study with the balloon time series are specifically performed so as to deal with realistic temperature disturbances in the TTL: larger temperature fluctuations are generally associated with longer-period disturbances, and large temperature fluctuations with periods below 10 min are thus very unlikely.

3. ***Reviewer*** — A related issue, and maybe the most significant one, is the selection of the initial conditions. All runs start on the verge of ice nucleation $S_0 \sim 150\,\%$. It is unrealistic to assume that each parcel starts from a very high supersaturation. One may ask, how do these parcels become such highly supersaturated in the first place? Starting from 100 % would any of the vertical velocity time series tested result in cloud formation? From the shape of the temperature perturbation profiles

in Fig. 4 it seems that they wouldn't. In reality there must be some underlying vertical movement bringing the supersaturation up to the initial conditions selected by the authors. Such movement (disregarded by the authors) is the actual driver of cloud formation, not the superimposed vertical velocity fluctuations. The analysis based only on the latter is flawed.

Authors — The reviewer noted that the initial saturation is equal to the saturation threshold S_0 and thus is unrealistically high in all of our simulations. This is actually not the case; our calculation begins at $t \leq t_0$ (where t_0 is the time at which nucleation begins) and with $S \leq S_0$ initially. In fact, most of the cases shown in Fig. 4 are with $S = 100\,\%$ initially. This misunderstanding arises perhaps because the evolution of the saturation ratio S is shown only for $t \geq t_0$ in Fig. 4. Please note that the subscript zero (e.g. t_0) denotes the time at which nucleation begins, which may not be the initial time of the parcel calculation.

The initial water vapour content and thus the initial saturation ratio of the air parcels is a free parameter in the simulations, and we have discussed the sensitivity of nucleation to this in Sect. 5.3 of the manuscript. This free parameter is meant to implicitly represent the large-scale ascent of air parcels in the TTL, which is, as noted by the reviewer, a prerequisite to high supersaturation. Lagrangian trajectory calculations show that air detrained from convection at or below saturation level takes typically several days to reach the supersaturation threshold for nucleation. On the other hand, nucleation itself occurs over a time scale of a few minutes to less than half an hour (depending on the chosen nucleation threshold). We exploit this scale separation to study the nucleation event and its sensitivity to high-frequency dynamical fluctuations once nucleation has started. It is implicit that the fluid parcel must previously be led to the verge of nucleation by large-scale motion in cloud free air but there is no point of studying this stage with our model. This will be mentioned in the revised version.

4. ***Reviewer*** — The authors omit important works (and in fact repeat some of the conclusions of those works) that may have helped in their analysis (e.g. Barahona and Nenes, 2011; Jensen et al., 2010, 2012; Cziczo et al., 2013; Murphy, 2014; Shi et al., 2015). For example, just as in this work, other works have shown (e.g. Jensen et al., 2010) that homogeneous nucleation could produce both, low and high ice crystal concentration. Similarly, field campaigns (e.g. Krämer et al., 2009) show high and low number concentration of ice crystals. Any comparison between field campaign data and model results should be done on a statistical basis. A limited set of parcel model simulations over very restricted conditions should not be used to draw conclusions on real clouds. Other aspects of the problem should be evaluated as well. Could the authors setup not only reproduce low crystal numbers but also the sustained clear-sky supersaturation and the small ice crystal size of TTL cirrus?

   Authors — Thank you for mentioning these references. We did cite about half of them and will improve our citation in the revised version. Jensen et al. (2010) and others have indeed shown that homogeneous nucleation could produce both high and low INCs. However, to our understanding, their explanation is based on a one-to-one relationship between cooling rates and INCs. In agreement with Spichtinger and Krämer (2013), we show that non-constant cooling rates break this one-to-one relationship. Our (new) contribution is that we provide the theoretical framework to explain the numerical results for non-constant (and constant) cooling rates, including

the classification of the two types of nucleation events, and the analytical relationship between N_i and $\triangle S$ (or $\triangle T$).

Our goal here is not to perform a detailed comparison with observations, which would certainly require much more complex microphysical models. We wish only to stress that some of our main findings, e.g. the large sensitivity of nucleated INCs to initial relative humidity in the presence of high-frequency motions, may give a clue for understanding the observed variability of INC in the TTL.

We are focusing only on ice nucleation process. Clear-sky supersaturation is an issue which is beyond the scope of this paper.

5. ***Reviewer*** — Line 11, page 8771. Such high vertical velocities are not shown.

   Authors — Our results indeed show that low INCs can be obtained for high vertical velocity w if w does not remain consistently high throughout the duration of the nucleation events. As shown in Fig. 1 below, the INC obtained when w decreases with time is much smaller than if w remains constant throughout nucleation. We have also illustrated this concept and shown values of w for the idealised temperature time series in Sect. 4.2. Please see also Fig. 3 in our reply to Reviewer 1 for more values of w in the balloon data.

6. ***Reviewer*** — Line 15, page 8771. This conclusion has been already stated in several papers (e.g. Barahona and Nenes, 2011; Jensen et al., 2010; Murphy, 2014).

   Authors — To our understanding, none of these papers specifically address the issue of time-varying cooling rates during nucleation, or mention temperature-limit events (a concept first developed here).

7. ***Reviewer*** — Line 5–10, page 8773. A concentration of $100\,\mathrm{L}^{-1}$ is just a nominal number, not a threshold that defines a limit between homogeneous and heterogeneous ice nucleation. Further evidence of the predominance of heterogeneous ice nucleation comes from field campaign data (e.g. Cziczo et al., 2013).

   Authors — Indeed, we gave $100\,\mathrm{L}^{-1}$ here as a nominal number, and not a threshold that represents a limit between homogeneous and heterogeneous ice nucleation. We would like to say here that low INCs should not be considered as an argument against homogeneous nucleation. We did not mean to disregard heterogeneous nucleation.

8. ***Reviewer*** — Page 8774–8775. The authors should show a plot of the vertical velocity time series associated with these measurements. Also explain why measurements from only two balloons are assumed as representative of the dynamics of the TTL.

   Authors — Please see Fig. 1 below or Fig. 3 in our reply to Reviewer 1 for values of w.

   The time series of temperature from the balloon measurements are the closest among all observations to the fluctuations experienced by a moving air parcel. At the moment we can only exploit two flights from a limited campaign (more will be available in the future) but they accumulate more than 6 months of flight and travelled around the equator. This is quite a significant sampling of the TTL.

9. ***Reviewer*** — Page 8776, lines 15–20. This is an important issue. Many interesting dynamics occurs from the sedimentation of ice crystals (e.g. Barahona and Nenes, 2011; Murphy, 2014). In particular, sedimentation would allow the build up of enough

supersaturation for homogeneous ice nucleation to occur. Thus the assumption that sedimentation would further decrease ice crystal concentration is erroneous.

Authors — We meant that sedimentation reduces the INC strictly within each nucleation event. If nucleation occurs following ice sedimentation, then we will count this occurrence as a new event. This sentence causes more confusion than we intended and will be deleted from the revised manuscript.

10. ***Reviewer*** — Page 8777, lines 1–5. Water vapour variability does not necessarily result from temperature fluctuations. In fact field campaigns have shown that temperature fluctuations are only partially responsible for the generation of supersaturation in the TTL (Diao et al., 2014).

    Authors — Here we simply refers to Eq. (4), which indicates that for a chosen/fixed pressure, there is a one-to-one relationship between T_0 and r_0. It is not necessary to discuss the topics of water vapour variability here.

11. ***Reviewer*** — Page 8779, Sect. 4.2. It is not clear how supersaturation can be generated in the first place without some persistent cooling (see general comments).

    Authors — We did allow the air parcels to cool before nucleation begins at t_0. Please see our response to Point 3 above.

12. ***Reviewer*** — Page 8784, Eq. (20). It must be mentioned that this is only true for negligible ice crystal concentrations.

    Authors — Not necessarily, the only requirement is that temperature variations happen much faster than nucleation.

13. ***Reviewer*** — In reality what the authors are defining as "temperature-limit" events is just a low ice crystal concentration regime, and has been introduced before (Kärcher and Lohmann, 2002).

    Authors — Kärcher and Lohmann (2002) studied constant vertical velocities only. They rather distinguish between different types of vapor-limit events by the fast and slow growth regimes (please see their Fig. 2). They did not study temperature-limit events in which the vertical velocities and cooling rates vary with time.

14. ***Reviewer*** — Page 8786, Line 20–25. According to this, the processes bringing up supersaturation to the level used in the initial conditions are the actual control of ice nucleation (see general comments).

    Authors — We disagree with the reviewer. The cooling associated with ascent in the TTL is the first stage leading to cirrus formation. However, we show that the distribution of ice following nucleation depends on the temperature fluctuations during nucleation.

References

Barahona, D. and Nenes, A.: Dynamical states of low temperature cirrus, Atmos. Chem. Phys., 11, 3757–3771, doi:10.5194/acp-11-3757-2011, 2011.

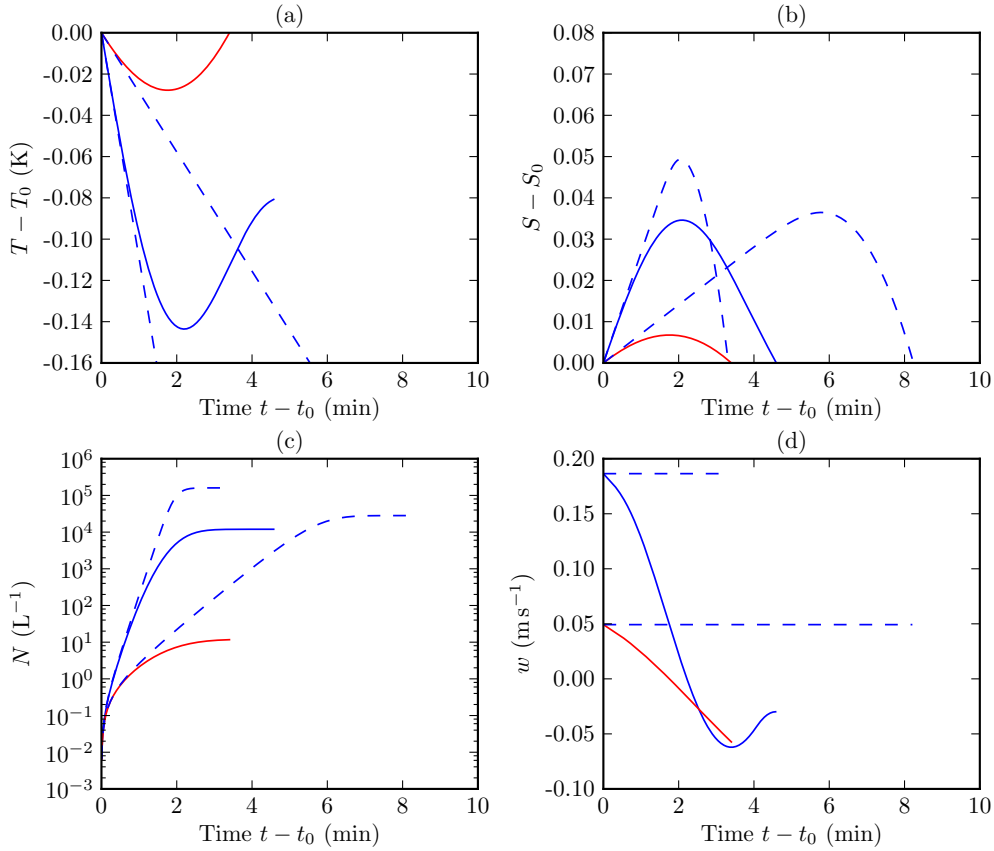

Figure 1: Evolution of temperature, saturation ratio, INC, and vertical velocity during nucleation events simulated using our model. The two solid curves show nucleation events forced by the balloon temperature data, and the two dash curves show the evolution if w remains constant throughout nucleation. Blue curves show vapour-limit events and red curves show temperature-limit events.

Cziczo, D. J., Froyd, K. D., Hoose, C., Jensen, E. J., Diao, M., Zondlo, M. A., Smith, J. B., Twohy, C. H., and Murphy, D. M.: Clarifying the dominant sources and mechanisms of cirrus cloud formation., Science, 340, 1320–1324, doi: 10.1126/science.1234145, 2013.

Jensen, E. J., Pfister, L., Bui, T.-P., Lawson, P., and Baumgardner, D.: Ice nucleation and cloud microphysical properties in tropical tropopause layer cirrus, Atmos. Chem. Phys., 10, 1369–1384, doi:10.5194/acp-10-1369-2010, 2010.

Jensen, E. J., Pfister, L., and Bui, T. P.: Physical processes controlling ice concentrations in cold cirrus near the tropical tropopause, J. Geophys. Res., 117, D11 205, doi:10.1029/2011JD017319, 2012.

Kärcher, B. and Lohmann, U.: A parameterization of cirrus cloud formation: Homogeneous freezing of supercooled aerosols, J. Geophys. Res., 107, D2, doi: 10.1029/2001JD000470, 2002.

Krämer, M., Schiller, C., Afchine, A., Bauer, R., Gensch, I., Mangold, A., Schlicht, S., Spelten, N., Sitnikov, N., Borrmann, S., de Reus, M., and Spichtinger, P.: Ice supersaturations and cirrus cloud crystal numbers, Atmos. Chem. Phys., 9, 3505–3522, doi:10.5194/acp-9-3505-2009, 2009.

Murphy, D. M.: Rare temperature histories and cirrus ice number density in a parcel and one-dimensional model, Atmos. Chem. Phys. Discuss., 14, 10 701–10 723, doi: 10.5194/acpd-14-10701-2014, 2014.

Shi, X., Liu, X., and Zhang, K.: Effects of preexisting ice crystals on cirrus clouds and comparison between different ice nucleation parameterizations with the Community Atmosphere Model (CAM5), Atmos. Chem. Phys., 15, 1503–1520, doi: 10.5194/acp-15-1503-2015, 2015.

Spichtinger, P. and Krämer, M.: Tropical tropopause ice clouds: a dynamic approach to the mystery of low crystal numbers, Atmos. Chem. Phys., 13, 9801–9818, doi: 10.5194/acp-13-9801-2013, 2013.

Effect of gravity wave temperature fluctuations on homogeneous ice nucleation in the tropical tropopause layer

August 12, 2015

We would like to thank the reviewer for the insightful evaluation of our work, especially for pointing out the error in Eq. (17), which will be corrected in the revised manuscript. Please note that this error does not affect our conclusions. Below is our point-by-point reply to the reviewer's comments.

1. ***Reviewer*** — There is a fundamental error in Eq. (17). As far as I can see from the original reference, the logarithm of the nucleation rate is represented by a third order polynomial in $\triangle a_\mathrm{w} = a_\mathrm{w} - a_\mathrm{w}^\mathrm{i}$ and NOT in $S a_\mathrm{w}$ (at least with the implicit definitions of a_w and S). It is clear from simple calculations that $\triangle a_\mathrm{w} \neq S a_\mathrm{w}$, thus the derivation of Eqs. (18)–(20) is incorrect. Probably, it is possible to re-derive similar expressions. However, in the present state the calculations are wrong. I have to express here that the main conclusion of the study remains unchanged, although the theoretical interpretation must be clarified.

   Authors — Thank you very much for pointing out this error in our derivation. Indeed

$$\triangle a_\mathrm{w} = a_\mathrm{w} - a_\mathrm{w}^\mathrm{i} = (S-1) a_\mathrm{w}^\mathrm{i} \tag{1}$$

   because $S = a_\mathrm{w}/a_\mathrm{w}^\mathrm{i}$. Thus Eq. (17) should be

$$\log_{10}(J) = P_3((S-1)a_\mathrm{w}^\mathrm{i}), \tag{2}$$

   and Eq. (18) becomes

$$\log_{10}(J_\mathrm{max}) = P_3((S_\mathrm{max}-1)a_\mathrm{w}^\mathrm{i}(T(t^*))) \approx P_3((S_0 + \triangle S - 1)a_w^\mathrm{i}(T_0)). \tag{3}$$

   The rest of the derivation and argument remain unchanged.

2. ***Reviewer*** — Although it is stated that beside the reference simulations with $T_0 = 195\,\mathrm{K}$ simulations with $T_0 = 180\,\mathrm{K}$ and $T_0 = 210\,\mathrm{K}$ were carried out, the representation of the results is quite minimalistic; they are just shown in Figs. 5/6. Maybe you should try to present the resulting (low!) ice crystal number concentrations in a kind of statistical matter. In addition you should try to scan the parameter space (T_0, p_0) in a bit finer resolution in order to have a better representation of the realistic cases. You should also try to compare these results at least qualitatively with measurements, e.g. as shown in Spichtinger and Krämer (2013).

Authors — The dependence on T_0 is monotonic, with the theoretical curve for $T_0 = 195\,\mathrm{K}$ lies between the curves for $T_0 = 180\,\mathrm{K}$ and $T_0 = 210\,\mathrm{K}$ (please see Figs. 5 and 6 in the manuscript). Calculations with other values of T_0 confirm this monotonic behaviour. Thus we do not feel it is necessary to add figures with other values of T_0 to the revised manuscript.

We have in fact received several requests from colleagues and readers of the manuscript to provide statistical comparison with observations. After long discussions among ourselves we decided not to do so because this study applies only to the nucleation period (which is very short, on the orders of minutes) at the beginning of the cloud lifetime. Since TTL cirrus may persist over a few days, observations typically do not capture the nucleation period of the clouds. Thus, a direct comparison between our simulations and observations may be somewhat misleading.

3. ***Reviewer*** — A major issue for the formation of low ice crystal number concentrations in the study by Spichtinger and Krämer (2013) was the occurrence of very slow background updrafts on order of $0.01\,\mathrm{m\,s^{-1}}$. You should try to use such background velocity fields for your realistic trajectory simulation.

   Authors — The updrafts used in our simulations are derived directly from the observed balloon temperature time series, and representative values are shown in Fig. 3 in our reply to Reviewer 1. They include both high-frequency motions with periods of several minutes (referred to as the wave component in Spichtinger and Krämer, 2013), and longer timescale motions (periods of several hours) that correspond to the "large-scale" component in Spichtinger and Krämer (2013). In our simulations, low INCs can be obtained even though our updraft velocities are typically much larger than $0.01\,\mathrm{m\,s^{-1}}$ (please see Fig. 3 in our reply to Reviewer 1).

4. ***Reviewer*** — There should be more accurate definitions of the used quantities. For instance, S is never defined although I assume that S is the saturation ratio with respect to ice. Also the scale height is not well-defined, is it the usual value $H \sim 8\,\mathrm{km}$?

   Authors — S is indeed the saturation ratio with respect to ice. The scale height H is typically 6 km in the tropical UT/LS. We will clarify these in the revised manuscript.

5. ***Reviewer*** — Page 8774, line 16: How reasonable is the time resolution of the trajectories in order to get a good representation of the relevant small-scale gravity waves? Please explain this in relation to the frequency of gravity waves, which might be expected.

   Authors — In principle, the balloon sampling rate (30 s, i.e. Nyquist frequency of $1\,\mathrm{min^{-1}}$) is sufficient to resolve all gravity waves (as well as higher frequency turbulence). However, to account for the balloon neutral oscillations at a period of 4 min, we had to filter the data using a high cut-off frequency (f_{high}). The representation of the gravity wave spectrum in the filtered data depends on the cut-off frequency rather than the original sampling rate. Please see our reply to Reviewer 1 for detailed discussions about our choice of f_{high} and the implication for the resolved gravity wave spectrum.

6. ***Reviewer*** — Page 8775, lines 5–7: Which resolution of ECMWF data is used for deriving the background temperature profile? Is it good enough for your considerations?

Authors — We used the highest vertical resolution provided by ECMWF, which is $\lesssim 500\,\mathrm{m}$ in the TTL. This spacing is sufficient to resolve the salient features of the background temperature profile, and thus to provide reasonable values for the lapse rate.

7. ***Reviewer*** — For the background aerosol (heterogeneous IN concentrations, aerosol particles for homogeneous nucleation) you often quote measurement studies, which were carried out mostly in the extratropics; since you want to address tropical tropopause layer, you should make clear that these measurement values are also reasonable for this tropical study.

   Authors — In the revised manuscript we will add another reference for aerosol observations, which included measurements in the tropics (Hermann et al., 2003). The properties of the background aerosols used in our simulations are within the range reported by Hermann et al. (2003).

8. ***Reviewer*** — Sedimentation of ice crystals is not just the effect of removal of ice crystal number concentrations; in combination with other processes (nucleation and diffusional growth) a kind of dynamic equilibrium might occur (see e.g. investigations by Spichtinger and Cziczo, 2010; Wacker, 1995). Probably for your simulations it is okay to omit sedimentation, but you should motivate this in a more convincing way, e.g. arguing about terminal velocities of very small ice crystals.

   Authors — The impact of sedimentation is indeed beyond the scope of this paper. Lagrangian parcel models (such as used in this work) are inadequate to fully address the impact of sedimentation. The sentence on lines 17–19, page 8776 will be deleted as it has caused more confusion than we intended.

9. ***Reviewer*** — The accommodation coefficient for the reference case seems a bit low ($\alpha = 0.05$). Skrotzki et al. (2013) indicate that the usual values are more in the range ($0.1 \leq \alpha \leq 1$). How large is the difference in the simulations between e.g. $\alpha = 0.5$ and simulations with $\alpha = 0.05$?

   Authors — We will use $\alpha = 0.1$ for the reference case in the revised manuscript. The results for the range of α between 0.001 and 1 are shown Figure 4 in our reply to Reviewer 1 and Fig. 7 in the manuscript. Please note that α affects vapour-limit events but not temperature-limit events.

10. ***Reviewer*** — I think your lower boundary of the nucleation rate J_ε is quite small, i.e. the probability of freezing a typical solution droplet at these conditions is probably zero (with respect to machine epsilon).

    Authors — In the revised manuscript we will use $J_\varepsilon = 10^9\,\mathrm{L^{-1}\,s^{-1}}$, compared with the original value of $1\,\mathrm{L^{-1}\,s^{-1}}$. Please see the discussions about J_ε in our reply to Reviewer 1.

11. ***Reviewer*** — It would be nice to add the time evolution of the nucleation rate for the different scenarios in Fig. 3; this would help to understand why the ice crystal number concentration is changed that drastically.

    Authors — The nucleation rate is

$$J = 10^{P_3((S-1)a_{\mathrm{w}}^{\mathrm{i}})} \tag{4}$$

(see Eq. 2 above) and thus it changes with time similarly to S. Since we have shown the evolution of S, we think it is not necessary to provide a separate figure for $J(t)$.

12. ***Reviewer*** — Page 8780, lines 14–23: I not understand what you want to say, please explain this in more details.

    Authors — These sensences are indeed confusing and will be removed from the manuscript.

13. ***Reviewer*** — The figures are quite hard to read. Actually, the figure captions could be extended. In Fig. 3 the different curves (all represented with the same colour, i.e. blue or red) should be labelled.

    Authors — Thanks. We will add labels to this figure in the revised manuscript.

References

Chen, Y., Kreidenweis, S. M., McInnes, L. M., Rogers, D. C., and DeMott, P. J.: Single particle analyses of ice nucleating aerosols in the upper troposphere and lower stratosphere, Geophys. Res. Lett., 25, 1391–1394, doi:10.1029/97GL03261, 1998.

Hermann, M., Zahn, A., Heinrich, G., and Brenninkmeijer, C. A. M.: Meridional distributions of aerosol particle number concentrations in the upper troposphere and lower stratosphere obtained by Civil Aircraft for Regular Investigation of the Atmosphere Based on an Instrument Container (CARIBIC) flights, J. Geophys. Res., 108, D3, doi: 10.1029/2001JD001077, 2003.

Skrotzki, J., Connolly, P., Schnaiter, M., Saathoff, H., Möhler, O., Wagner, R., Niemand, M., Ebert, V., and Leisner, T.: The accommodation coefficient of water molecules on ice â cirrus cloud studies at the AIDA simulation chamber, Atmos. Chem. Phys., 13, 4451–4466, doi:10.5194/acp-13-4451-2013, 2013.

Spichtinger, P. and Cziczo, D. J.: Impact of heterogeneous ice nuclei on homogeneous freezing events in cirrus clouds, J. Geophys. Res., 115, D14 208, doi:10.1029/2009JD012168, 2010.

Spichtinger, P. and Krämer, M.: Tropical tropopause ice clouds: a dynamic approach to the mystery of low crystal numbers, Atmos. Chem. Phys., 13, 9801–9818, doi:10.5194/acp-13-9801-2013, 2013.

Wacker, U.: Competition of Precipitation Particles in a Model with Parameterized Cloud Microphysics, J. Atmos. Sci., 52, 2577–2589, doi:10.1175/1520-0469(1995)052<2577:COPPIA>2.0.CO;2, 1995.

Manuscript prepared for Atmos. Chem. Phys.
with version 2014/07/29 7.12 Copernicus papers of the LaTeX class copernicus.cls.
Date: 12 August 2015

Effect of gravity wave temperature fluctuations on homogeneous ice nucleation in the tropical tropopause layer

T. Dinh[1], **A. Podglajen**[2], **A. Hertzog**[2], **B. Legras**[3], **and R. Plougonven**[2]

[1]Program in Atmospheric and Oceanic Sciences, Princeton University, Princeton, New Jersey, USA
[2]Laboratoire de Météorologie Dynamique, École Polytechnique, Palaiseau, France
[3]Laboratoire de Météorologie Dynamique, École Normale Supérieure, Paris, France

Correspondence to: T. Dinh (tdinh@princeton.edu)

Abstract. The impact of high-frequency fluctuations of temperature on homogeneous nucleation of ice crystals in the vicinity of the tropical tropopause is investigated using a bin microphysics scheme for air parcels. The imposed temperature fluctuations come from measurements during isopycnic balloon flights near the tropical tropopause. The balloons collected data at high frequency, guaranteeing that gravity wave signals are well resolved.

With the observed temperature time series, the numerical simulations with homogeneous freezing show a full range of ice number concentration (INC) as previously observed in the tropical upper troposphere. In particular, a low INC may be obtained if the gravity wave perturbations produce a non-persistent cooling rate (even with large magnitude) such that the absolute change in temperature remains small during nucleation. This result is explained analytically by a dependence of the INC on the absolute drop in temperature (and not on the cooling rate). This work suggests that homogeneous ice nucleation is *not* necessarily inconsistent with observations of low INCs.

1 Introduction

Cirrus clouds have an important impact on the global radiative energy budget (Lohmann and Roeckner, 1995). In the tropical tropopause layer (TTL, Fueglistaler et al., 2009), cirrus clouds contribute to the radiative heating (Corti et al., 2006; Dinh and Fueglistaler, 2014a) and control the dehydration of the air before entry into the stratosphere (Brewer, 1949; Jensen et al., 1996; Dinh and Fueglistaler, 2014b). For all cirrus clouds, the radiative and climate impact, ability to modify water vapour, and cloud evolution are sensitive to the ice number concentration (e.g. Kärcher et al., 2014), which depends strongly on the nucleation process of ice crystals.

When evaluating the ice number concentration (INC) produced by nucleation, it has been often assumed that the relevant time scale is sufficiently short such that the vertical velocity and associated adiabatic cooling rate remain constant (e.g. Barahona and Nenes, 2008). For constant cooling rates, homogeneous freezing of aqueous aerosols produces higher INCs ($> 1000\,\mathrm{L}^{-1}$) than those commonly observed ($\lesssim 100\,\mathrm{L}^{-1}$) in cirrus clouds (Lawson et al., 2008; Krämer et al., 2009; Davis et al., 2010). Observations and calculations of INC based on homogeneous freezing can be reconciled only if very low vertical speeds ($w < 0.01\,\mathrm{m\,s}^{-1}$) are used in the simulations. This seems at odds with the ubiquitous presence of atmospheric gravity waves, which typically generate an order of magnitude larger disturbances in the vertical velocity. Therefore, it has been suggested that heterogeneous freezing (instead of homogeneous freezing) is the dominant nucleation mechanism for cirrus clouds in the upper troposphere (Jensen et al., 2010, 2012). The INC obtained by heterogeneous freezing is apparently limited by the availability of suitable ice nuclei (generally less than $100\,\mathrm{L}^{-1}$) in the upper troposphere (Chen et al., 1998; Rogers et al., 1998).

However, Spichtinger and Krämer (2013) pointed out that high-frequency variations in temperature and cooling rates can substantially decrease the INC produced during homogeneous nucleation compared to those obtained with constant updraft speeds. Yet, their numerical results are based on ideally constructed temperature time series, and so remain somewhat conceptual. The present work complements their study by using temperature time series data collected at high temporal resolution during long-duration balloon flights near the tropical tropopause. The observed temperatures contain

perturbations from a spectrum of atmospheric waves, with periods ranging from days to minutes. Our numerical simulations based on these observed temperature time series confirm the earlier results of Spichtinger and Krämer (2013).

In addition to the numerical simulations using realistic temperature time series (as described above), our contribution is to provide a theoretical framework for characterizing homogeneous nucleation while taking into account the temperature fluctuations due to gravity waves. The theoretical framework put forward here complements previous studies (see also Barahona and Nenes, 2011; Jensen et al., 2010, 2012; Murphy, 2014), where the effect of high-frequency temperature fluctuations on ice nucleation has been described but not explained analytically.

The article is organised as follows. Sections 2 and 3 describe the balloon data and the technical details of the model used here to simulate homogeneous ice nucleation. Section 4 presents the numerical results. Section 5 provides the theoretical basis explaining how the fluctuations in time of temperature may affect homogeneous ice nucleation. Section 6 contains the conclusions.

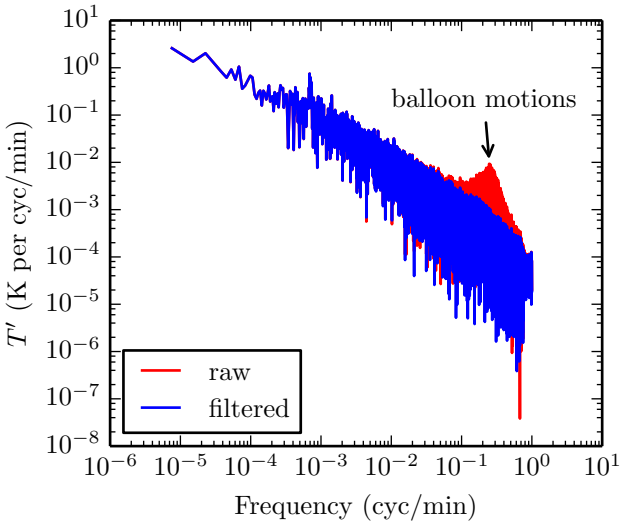

Figure 1. Power spectrum of the raw and filtered temperature perturbation time series derived from the balloon vertical displacements.

2 Balloon data descriptions

The temperature time series used in this study are derived from data collected by two long-duration, superpressure balloons launched by the French Space Agency from Seychelles Islands (55.5° E, 4.6° N) in February 2010 in the framework of the Pre-Concordiasi campaign (Rabier et al., 2010). The balloons flew at an altitude of about 19 km, and achieved circumterrestrial flights, therefore sampling the whole equatorial circle. Details on the balloon trajectories and large-scale atmospheric dynamics during the flights can be found in Podglajen et al. (2014). Superpressure balloons are advected by the wind on isopycnic (constant-density) surfaces and therefore behave as quasi-Lagrangian tracers of atmospheric motions. A further remarkable property of superpressure balloons is their sensitivity to atmospheric gravity waves (Massman, 1978; Nastrom, 1980; Boccara et al., 2008; Vincent and Hertzog, 2014). The sampling frequency of the balloon position, atmospheric pressure and temperature during the campaign is every 30 s.

Here, we do not use the temperature observations gathered during the flights to constrain the nucleation simulations; these time series tend to be both too noisy and warm biased during daytime. Instead, we infer the temperature disturbances from the balloon vertical displacements ($\zeta'_{\rm b}$). The isentropic air parcel vertical displacement (ζ') is linked to that of the isopycnic balloon through

$$\zeta' = \frac{g/c_p + \partial\overline{T}/\partial z}{g/R_{\rm a} + \partial\overline{T}/\partial z}\,\zeta'_{\rm b} \qquad (1)$$

(Boccara et al., 2008), where g is the gravitational acceleration, c_p is the specific heat at constant pressure, $R_{\rm a}$ is the gas constant for air, and $\partial\overline{T}/\partial z$ is the vertical gradient of the background temperature. We use the European Centre for Medium-Range Weather Forecasts (ECMWF) operational analyses to diagnose $\partial\overline{T}/\partial z$ at the balloon position in the above equation. The isentropic vertical displacement is then converted to the Lagrangian temperature fluctuation (felt by the air parcel) at the balloon flight level (i.e. in the lower stratosphere) by

$$T'_{\rm LS} = -\frac{g}{c_p}\,\zeta'. \qquad (2)$$

We must furthermore take into account that the balloons flew in the lower stratosphere rather than in the upper troposphere where most of the cirrus form. Because of the difference in stability of these two regions, the vertical displacements and hence temperature fluctuations induced by gravity waves are larger in the upper troposphere than in the lower stratosphere. For conservative wave propagation, it can be shown that:

$$T'_{\rm UT} = \sqrt{\frac{N_{\rm LS}}{N_{\rm UT}}}\,\exp\left(-\frac{\Delta z}{2H}\right)T'_{\rm LS}, \qquad (3)$$

where $N_{\rm UT}$ and $N_{\rm LS}$ respectively are the buoyancy frequencies in the upper troposphere and lower stratosphere, Δz is the difference between the balloon flight and cloud altitudes, H is the atmospheric scale height (~ 6 km in the TTL), and $T'_{\rm UT}$ is the temperature disturbance in the upper troposphere induced by the gravity wave packet observed at the balloon altitude. Typically, $N_{\rm LS} \sim 2N_{\rm UT}$, and $T'_{\rm UT} \sim T'_{\rm LS}$ if the cirrus forms 4 km below the balloon flight level.

The power spectrum of the temperature perturbation ($T'_{\rm UT}$) time series derived from the balloon vertical displacements is

shown in Fig. 1. Notice that the balloon neutral oscillations due to the flight mechanics have a frequency of $0.25\,\mathrm{min}^{-1}$. Since the spectrum of gravity waves extends up to the Brunt–Väisälä frequency (typically less than $0.20\,\mathrm{min}^{-1}$ in the TTL), we expect that the balloon motions does not negatively affect the quality of gravity waves in the dataset. Nevertheless, we applied a butterworth band-stop filter to remove the balloon oscillations from the temperature time series (Fig. 1). We have also experimented filtering the data using a high cut-off frequency of 0.10 or $0.20\,\mathrm{min}^{-1}$ (not shown). Our simulations (Sect. 4) are not sensitive to the data filtering method.

3 Model configurations

We compute homogeneous freezing of aqueous aerosols following Koop et al. (2000), and depositional growth of ice crystals (see e.g. Pruppacher and Klett, 1978) using the bin scheme designed by Dinh and Durran (2012). The formula for the water activity has been revised following Koop and Zobrist (2009). The saturation water vapour pressure (over ice) is taken from Murphy and Koop (2005).

Ice crystals and aerosol particles that form ice crystals are assumed to be spherical. We use 20 bins to resolve the size distribution of ice crystals with radii up to $10\,\mu\mathrm{m}$. The time step used in the simulations is 0.5 s. The numerical results do not change with more bins or smaller time step, i.e. the stated bin and time resolutions are sufficient to ensure accuracy.

The number concentration of the aerosol reservoir is $N_\mathrm{a} = 200\,\mathrm{cm}^{-3}$, and aerosol particles are assumed to be monodispersed in size with a radius of $0.25\,\mu\mathrm{m}$. These assumptions are within observed properties of aerosols in the upper troposphere (Chen et al., 1998; Hermann et al., 2003). Simulations with polydispersed aerosols up to $1\,\mu\mathrm{m}$ in size do not show qualitative differences, and so we retain a monodispersed distribution to simplify the analytical derivation in Sect. 5.

In addition, we do not consider ice sedimentation in order to focus solely on the nucleation process. Further, nucleation is calculated only for initially ice-free air parcels. The effect of pre-existing ice on nucleation has been discussed elsewhere (see Shi et al., 2015).

Currently, there is not yet a well constrained limit on the deposition coefficient (also called accommodation coefficient). The deposition coefficient controls the number of gas molecules that effectively enter the condensed phase after a collision with the ice surface. Laboratory measurements of the deposition coefficient vary by as much as three orders of magnitude, between 0.001 and 1 (Magee et al., 2006; Skrotzki et al., 2013). Figure 2 illustrates the effect of varying the deposition coefficient α on the INC calculated using our model. For the same constant updraft, the INC obtained by homogeneous nucleation is smaller for larger α. In the following sections, we first present the simulations for $\alpha = 0.1$ and then discuss the sensitivity to α in Sects. 4.3.3 and 5.2.

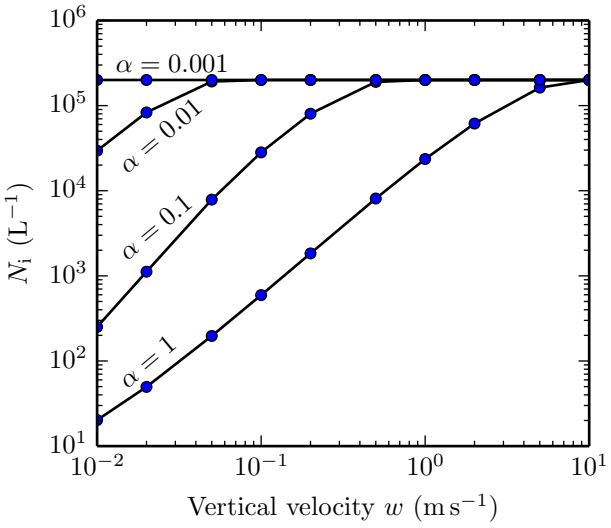

Figure 2. INC obtained from homogeneous nucleation at 195 K forced by constant vertical velocity w for different values of the deposition coefficient α.

4 Numerical simulations

For adiabatic motions, the effect of pressure variations on the water vapour mixing ratio (r) can be neglected compared with that due to temperature variations. Assuming constant air pressure, we prescribe an initial water vapour content for the air parcels such that nucleation occurs at a chosen temperature T_0. This is possible because the saturation ratio with respect to ice (S) at the threshold of nucleation (S_nuc) is a function of temperature (Koop et al., 2000; Kärcher and Lohmann, 2002; Ren and Mackenzie, 2005), and it is related to the initial water vapour mixing ratio of air parcels by

$$r_0 = \frac{e_\mathrm{sat}(T_0) S_\mathrm{nuc}(T_0)}{p} \frac{R_\mathrm{a}}{R_\mathrm{v}}, \tag{4}$$

where p is air pressure, e_sat is the saturation water vapour pressure over ice, and R_a and R_v are respectively the gas constants of air and water vapour. The notations $e_\mathrm{sat}(T_0)$ and $S_\mathrm{nuc}(T_0) \equiv S_0$ refer to respectively e_sat and S_nuc at T_0. Note that, up to the nucleation time the vapour mixing ratio r is conserved. As illustrated in Fig. 3, every air parcel follows an isoline of constant water vapour mixing ratio ($r = r_0$) until crossing the $S_\mathrm{nuc}(T)$ curve, at which point nucleation begins.

The simulations were first carried out for pressure $p = 100\,\mathrm{hPa}$, nucleation temperature $T_0 = 195\,\mathrm{K}$, and deposition coefficient $\alpha = 0.1$ (Sects. 4.1, 4.2, and 4.3.1). A nucleation event is defined to start when the rate of nucleation exceeds a threshold J_ε, and to end when it becomes less than J_ε. For our simulations, choosing a threshold of $J_\varepsilon = 10^9\,\mathrm{L}^{-1}\,\mathrm{s}^{-1}$, we have $S_0 = 1.553$ for $T_0 = 195\,\mathrm{K}$. Sensitivities to T_0 in the range between 180 and 210 K, and α in the range between 0.001 and 1 are discussed in Sects. 4.3.2 and 4.3.3.

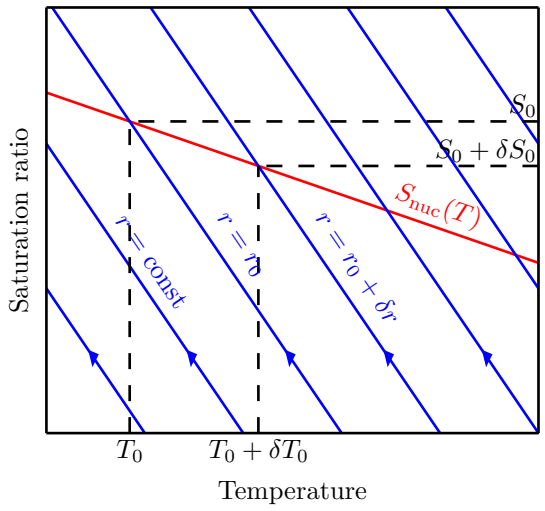

Figure 3. Diagram illustrating the initial conditions of the air parcels. Prior to nucleation air parcels follow isolines of water vapour mixing ratio r (shown here in blue) and approach the curve $S_{\rm nuc}(T)$ from below (as indicated by the arrows). Nucleation begins at the intersections of the r isolines with the curve $S_{\rm nuc}(T)$.

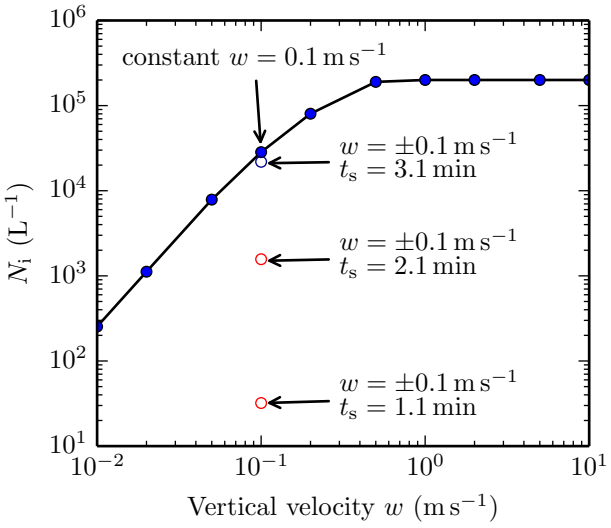

Figure 4. INCs obtained for $\alpha = 0.1$ with constant w (filled circles), and with $w = \pm 0.1\,\mathrm{m\,s^{-1}}$ (open circles), see Eq. (7). Vapour-limit events are shown in blue and temperature-limit events are shown in red.

Time series of temperature is defined by

$$T(t) = T_0 + T'(t), \tag{5}$$

where $T'(t)$ are either idealised following temperature variations associated with constant and time-varying vertical velocities (Sects. 4.1 and 4.2), or taken from the balloon data (Sect. 4.3).

4.1 Constant vertical velocity

Here temperature is set to decrease with time due to adiabatic cooling at a constant vertical velocity in a hydrostatic background, i.e.

$$T'(t) = -\frac{g}{c_p} w t. \tag{6}$$

For $\alpha = 0.1$, the number of ice crystals nucleated $N_{\rm i}$ increases with w if $w < 1\,\mathrm{m\,s^{-1}}$ (see Fig. 4). For $w \geq 1\,\mathrm{m\,s^{-1}}$, all aerosols particles form ice, hence $N_{\rm i} = N_{\rm a} = 200\,\mathrm{cm^{-3}}$. Figure 4 shows that if the vertical velocity and the cooling rate are constant during the nucleation events, w must be less than $0.01\,\mathrm{m\,s^{-1}}$ in order that $N_{\rm i} < 100\,\mathrm{L^{-1}}$. This result is consistent with previous studies (e.g. Krämer et al., 2009) of homogeneous freezing under constant vertical velocity.

4.2 Nonpersistent cooling

Now we vary w with time so that the rate of change of temperature $\frac{\mathrm{d}T}{\mathrm{d}t}$ is no longer constant with time. Specifically, we set

$$w(t) = \begin{cases} +0.1\,\mathrm{m\,s^{-1}} & \text{if } t \leq t_{\rm s}, \\ -0.1\,\mathrm{m\,s^{-1}} & \text{if } t > t_{\rm s}. \end{cases} \tag{7}$$

The time $t_{\rm s}$ at which w switches signs is varied by setting $t_{\rm s} = \{1.10; 2.10; 3.10\}$ min. The dash lines in Fig. 5 show the evolution of the vertical velocity, temperature, saturation ratio, and INC during the nucleation events forced by $w = \pm 0.1\,\mathrm{m\,s^{-1}}$ as defined above.

In the event where w switches signs at $t_{\rm s} = 3.10$ min (blue dash curves in Fig. 5), the saturation ratio (S) reaches a maximum ($S_{\rm max}$) at $t^* = 3.05$ min, which is before the minimum temperature ($T_{\rm min}$) is reached ($t^* < t_{\rm s}$). Here, $S_{\rm max}$ is controlled by the depletion of water vapour by depositional growth of ice crystals. The INC in this event is almost the same as that which would have been obtained if w were kept constant at $0.1\,\mathrm{m\,s^{-1}}$ (see also Fig. 4). We refer to this event and all cases with constant w as "vapour-limit," indicating that $N_{\rm i}$ is limited by the depletion of water vapour.

For the other two events in which w switches signs earlier at $t_{\rm s} = 1.10$ and 2.10 min (red curves in Fig. 5 and red circles in Fig. 4), $N_{\rm i}$ is significantly smaller than that obtained for the vapour-limit event described above. For these two events, $S_{\rm max}$ and $T_{\rm min}$ occur at the same time ($t^* = t_{\rm s}$). After $S_{\rm max}$ is reached, S decreases with time because temperature increases with time. We refer to these events as "temperature-limit" because the minimum temperature determines $S_{\rm max}$ and hence $N_{\rm i}$. The depletion of water vapour by ice depositional growth can be neglected because $N_{\rm i}$ is small.

The numerical results show that homogeneous nucleation may be cut off if the cooling that initiates nucleation does not persist sufficiently long into the nucleation events. As a con-

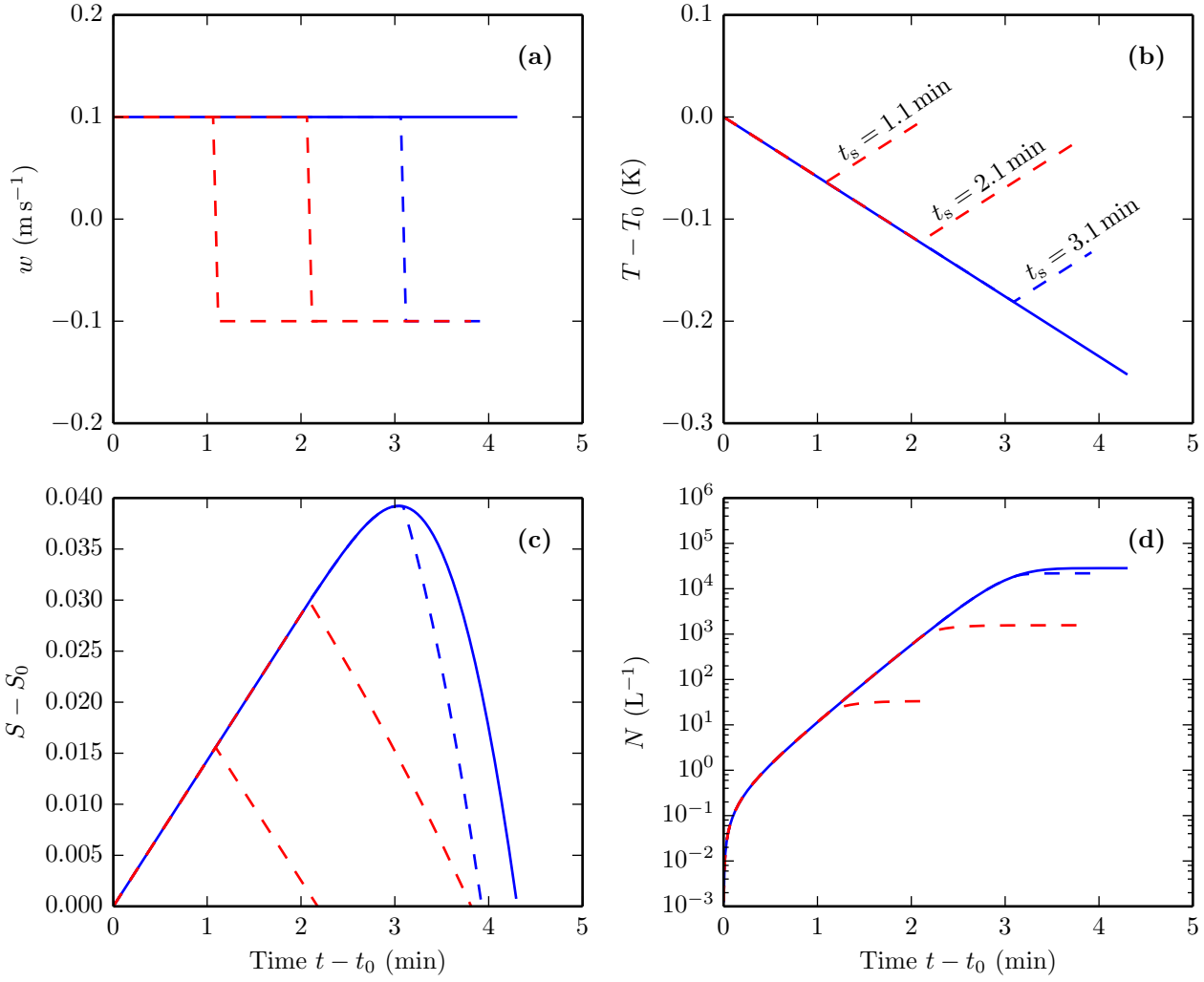

Figure 5. Evolution of vertical velocity **(a)**, temperature **(b)**, saturation ratio **(c)**, and INC **(d)** during nucleation events forced by constant $w = 0.1\,\mathrm{m\,s^{-1}}$ (solid) and by $w = \pm 0.1\,\mathrm{m\,s^{-1}}$ (dash) as defined by Eq. (7). Blue curves show vapour-limit events and red curves show temperature-limit events.

sequence, low INCs can be obtained for temperature-limit events despite initially high vertical velocities and cooling rates. The results in this section are consistent with the simulations with similar setups that have been carried out previously by Spichtinger and Krämer (2013).

4.3 Balloon temperature time series

In contrast to the previous sections which used theoretically constructed temperature time series, the numerical simulations presented in this section were carried out using the balloon data. Below, for Sect. 4.3.1 we use $T_0 = 195$ K and $\alpha = 0.1$ (same as previously in Sects. 4.1 and 4.2). In Sects. 4.3.2 and 4.3.3, we vary T_0 between 180 and 210 K, and α between 0.001 and 1 to explore sensitivities to these parameters.

4.3.1 Control simulations with $T_0 = 195$ K and $\alpha = 0.1$

The evolution of the saturation ratio and temperature during representative nucleation events simulated using the balloon data are shown in Fig. 6. The duration τ of the nucleation events simulated with the observed temperature data ranges from a few minutes up to about an hour. Because of the high-frequency fluctuations in the observed temperature time series, the cooling rate is typically not constant during a nucleation event. Moreover, more than one local maxima and minima in T and S may occur during one nucleation event. Nevertheless, it is possible to distinguish between

– vapour-limit events, for which the absolute maximum S_{max} is obtained before the absolute minimum T_{min} be-

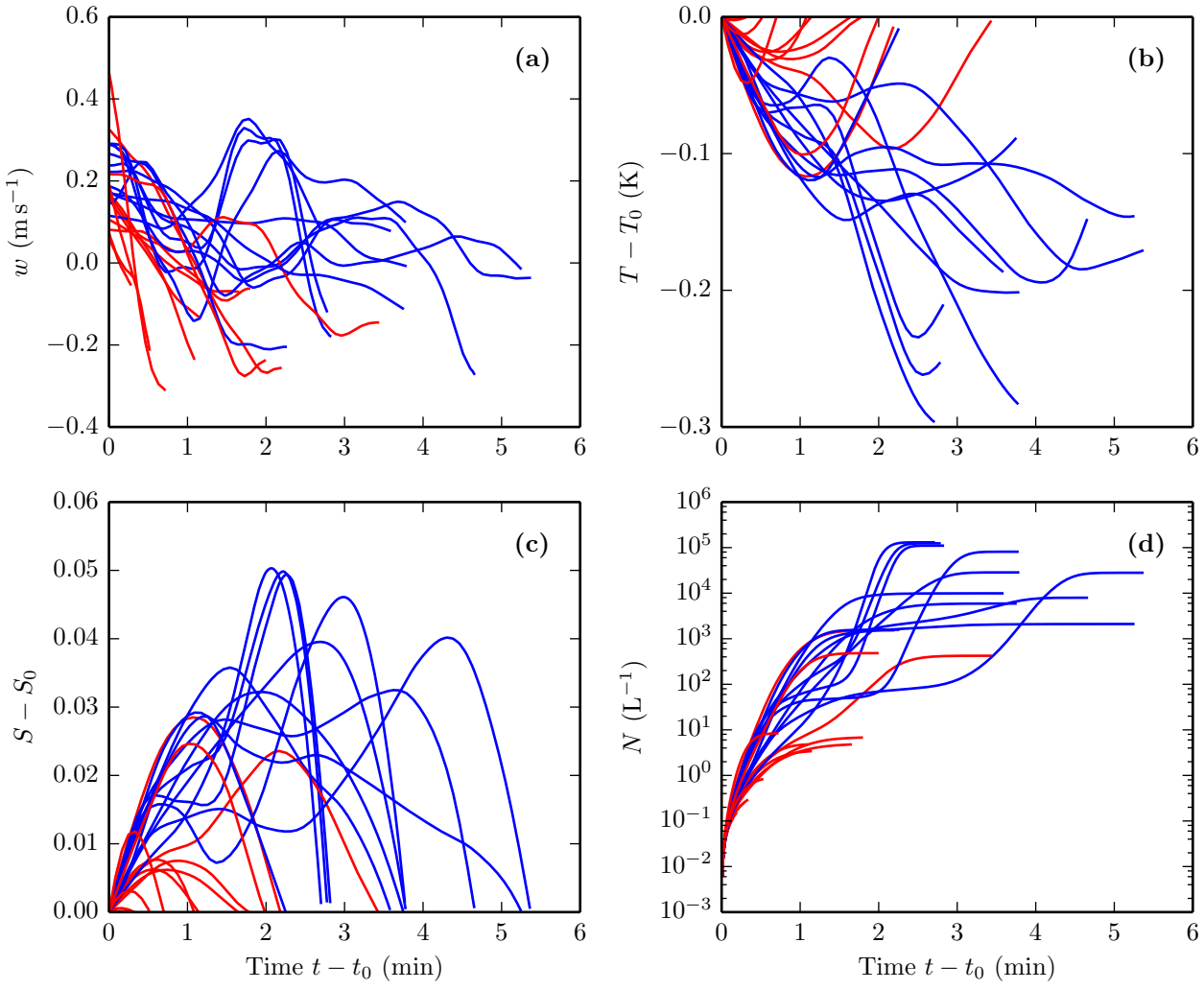

Figure 6. Evolution of vertical velocity **(a)**, temperature **(b)**, saturation ratio **(c)**, and INC **(d)** during representative nucleation events forced by the temperature perturbations derived from the balloon data. Blue curves show vapour-limit events and red curves show temperature-limit events.

cause of substantial vapour depletion; constant cooling rate is a special case of this type, and

– temperature-limit events, for which S_{max} is obtained at the same time as T_{min}; temperature controls the cutoff of nucleation, and vapour depletion is negligible.

As shown in Fig. 7, the INC nucleated during temperature-limit events is smaller than for vapour-limit events. The numerical results suggest that, for all nucleation events, N_i increases exponentially with the difference

$$\triangle S \equiv S_{max} - S_0 \tag{8}$$

as long as $N_i \ll N_a$ (Fig. 7). For temperature-limit nucleation events, N_i increases exponentially with $|\triangle T|$, where

$$\triangle T \equiv T_{min} - T_0. \tag{9}$$

4.3.2 Sensitivity of INC to nucleation temperature

Here, we prescribe the initial vapour content r_0 of the air parcels such that the nucleation temperature is either $T_0 =$ 180 or 210 K. In Fig. 3, this is equivalent to choosing another isoline of r and displacing accordingly the values of T_0 and S_0 at nucleation. As in the previous section, the balloon temperature perturbations are added to these nucleation temperatures to obtain the temperature time series $T(t)$, see Eq. (5).

The number of ice crystals nucleated for $T_0 = 180$ and 210 K is shown in Fig. 8. The data for $T_0 = 195$ K shown previously in Fig. 7 generally lie between the data points for $T_0 = 180$ and 210 K, that is, there is a monotonic relationship between N_i and T_0. For the same $\triangle S$, N_i is smaller for smaller T_0. Conversely, for the same $\triangle T$, N_i is smaller for larger T_0.

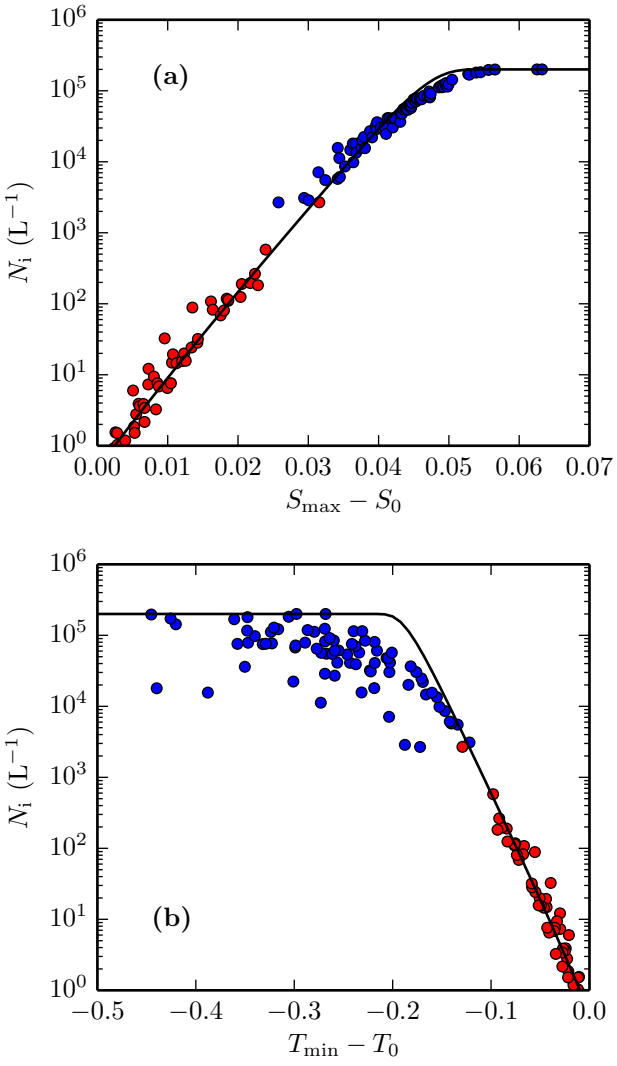

Figure 7. Number of ice crystals nucleated at $T_0 = 195\,\mathrm{K}$ for $\alpha = 0.1$ using the balloon temperature perturbation time series. Blue circles show vapour-limit nucleation events. Red circles show temperature-limit nucleation events. The solid curves are obtained from Eqs. (14)–(18) with $\mu = 0.05\,\mathrm{s}^{-1}$.

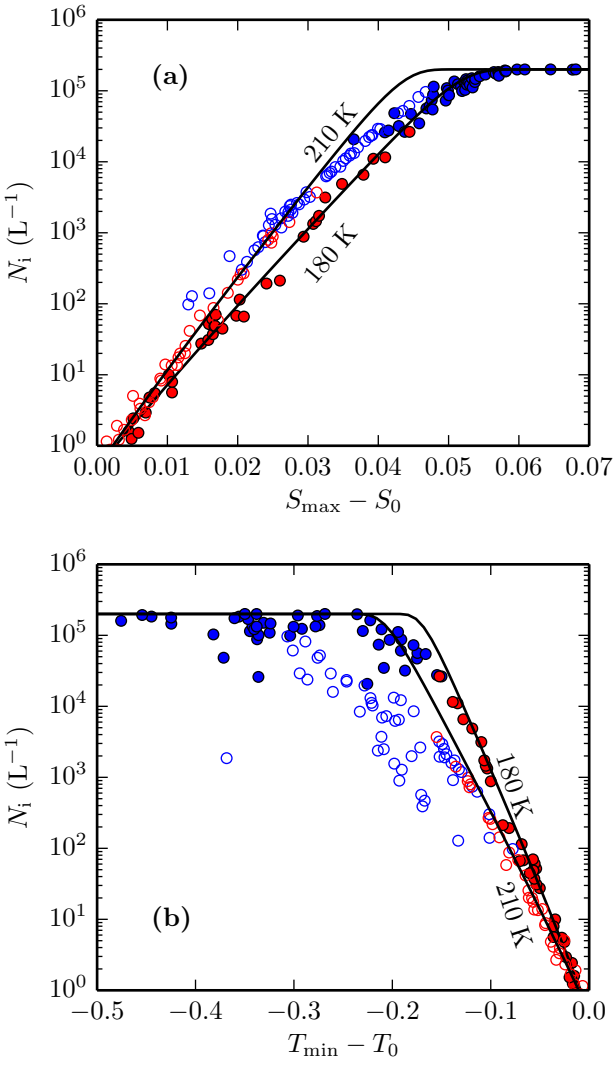

Figure 8. Same as Fig. 7 ($\alpha = 0.1$) but for $T_0 = 180\,\mathrm{K}$ (filled circles) and 210 K (empty circles).

4.3.3 Sensitivity of INC to deposition coefficient

The number of ice crystals nucleated at $T_0 = 195\,\mathrm{K}$ for $\alpha = 0.001$ and $\alpha = 1$ is shown in Fig. 9. Notice that the transition from temperature-limit events to vapour-limit events occurs at lower INC for $\alpha = 1$ than $\alpha = 0.001$. This makes sense because ice crystals deplete water vapour at a faster rate in the case $\alpha = 1$, and so the number of ice crystals needed to significantly deplete water vapour is smaller.

For temperature-limit events, the functional dependence of N_i on $\triangle S$ (or $\triangle T$) is invariant for different values of α, i.e. N_i is independent of α. However, for vapour-limit events, N_i is smaller for $\alpha = 1$ than $\alpha = 0.001$ for the same $\triangle S$ (or $\triangle T$). The sensitivity of vapour-limit events to the deposition coefficient is explained in the theory section below.

5 Theory and discussions

In this section we provide the theoretical basis that explains the numerical results shown previously in Sect. 4.

5.1 Formula for ice number concentration

The rate of nucleation of ice crystals during a nucleation event is given by

$$\frac{\mathrm{d}N}{\mathrm{d}t} = (N_\mathrm{a} - N) J V_\mathrm{a}, \tag{10}$$

where N_a is the aerosol particle number concentration, V_a is the volume of each aerosol particle, and J is the homoge-

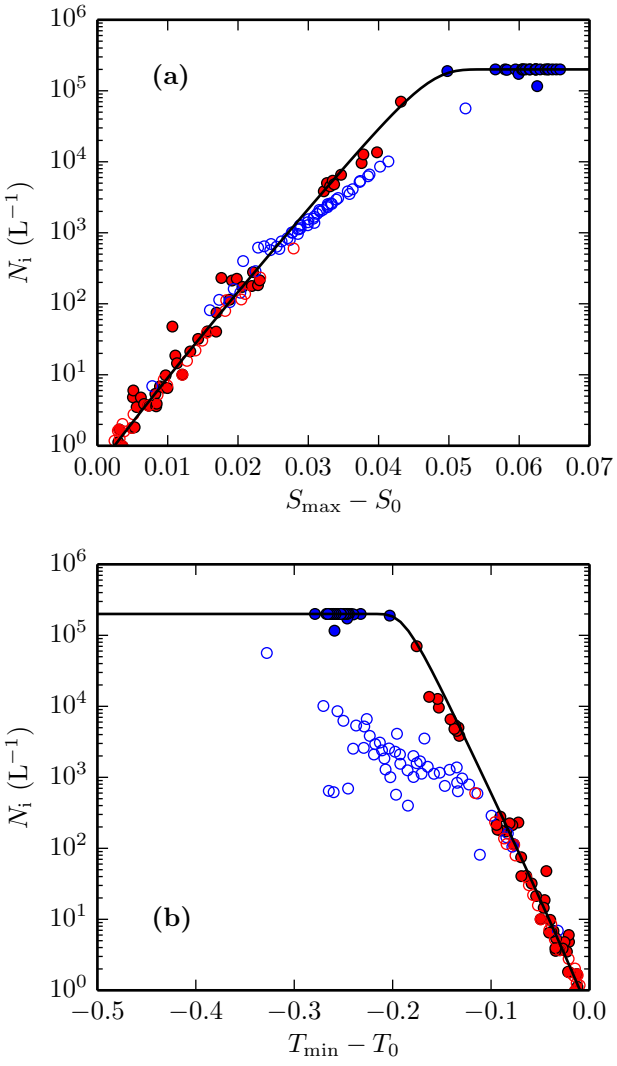

Figure 9. Same as Fig. 7 ($T_0 = 195$ K) but for $\alpha = 0.001$ (filled circles) and $\alpha = 1$ (empty circles).

neous nucleation rate given by Koop et al. (2000, their Eq. 7). By integrating Eq. (10) from the beginning ($t = t_0$) to end ($t = t_0 + \tau$) of the nucleation event we obtain

$$\ln\left(1 - \frac{N_i}{N_a}\right) = -V_a \int_{t_0}^{t_0+\tau} J \mathrm{d}t = -V_a J_{max} \int_{t_0}^{t_0+\tau} \exp(\ln(J) - \ln(J_{max}))\mathrm{d}t, \quad (11)$$

where $J_{max} \equiv J(t^*)$ is the maximum value of J during the nucleation event ($t_0 < t^* < t_0+\tau$), and $N_i \equiv N(t_0+\tau)$ is the INC obtained at the end of the nucleation event. Following the steepest descent method, we obtain

$$\begin{aligned}
&\ln\left(1 - \frac{N_i}{N_a}\right) \\
&\approx -V_a J_{max} \int_{t_0}^{t_0+\tau} \exp\left(\frac{1}{2}\frac{\mathrm{d}^2(\ln J)}{\mathrm{d}t^2}(t^*)(t-t^*)^2\right)\mathrm{d}t \\
&\approx -V_a J_{max} \int_{t_0-t^*}^{t_0+\tau-t^*} \exp(-\mu^2 t^2)\mathrm{d}t \\
&\approx -V_a J_{max} \int_{-\infty}^{\infty} \exp(-\mu^2 t^2)\mathrm{d}t \\
&\approx \sqrt{\pi} V_a \frac{J_{max}}{\mu}, \qquad (12)
\end{aligned}$$

where

$$\mu^2 = -\frac{1}{2}\frac{\mathrm{d}^2(\ln J)}{\mathrm{d}t^2}(t^*) = -\frac{1}{2J_{max}}\frac{\mathrm{d}^2 J}{\mathrm{d}t^2}(t^*). \quad (13)$$

The approximations used to derive Eq. (12) are appropriate if $t^* - t_0$ and $t_0 + \tau - t^*$ are both significantly larger than the e-folding time scale given by μ^{-1}. These criteria are well satisfied in our simulations. From Eq. (12) we obtain

$$N_i \approx N_a \left(1 - \exp\left(-\sqrt{\pi} V_a \frac{J_{max}}{\mu}\right)\right). \quad (14)$$

For homogeneous ice nucleation, J is given by (see Koop et al., 2000)

$$\log_{10}(J) = P_3((S-1)a_w^i), \quad (15)$$

where P_3 denotes a third order polynomial, and a_w^i is the water activity of a solution in equilibrium with ice, which is independent of the nature of the solute (Koop et al., 2000). It follows that

$$\begin{aligned}
\log_{10}(J_{max}) &= P_3((S_{max}-1)a_w^i(T(t^*))) \\
&\approx P_3((S_0 + \triangle S - 1)a_w^i(T_0)), \qquad (16)
\end{aligned}$$

where $\triangle S$ is the change in the saturation ratio during the nucleation event defined in Eq. (8). Since a_w^i and S_0 are both functions of temperature, J_{max} is a function of $\triangle S$ and temperature. Therefore, Eqs. (14) and (16) indicate that N_i is a function of $\triangle S$, μ, and temperature. However, note that $\triangle S$, μ, and temperature are not exclusively independent variables. In fact, substituting Eqs. (15) and (16) into Eq. (13) we obtain

$$\mu^2 \approx f(\triangle S, T_0)\left(\frac{\mathrm{d}^2 S}{\mathrm{d}t^2}(t^*)\right) + h(\triangle S, T_0)\left(\frac{\mathrm{d}^2 T}{\mathrm{d}t^2}(t^*)\right), \quad (17)$$

where $f(\triangle S, T_0)$ and $h(\triangle S, T_0)$ are functions of $\triangle S$ and T_0, and we have made the approximation that $T \approx T_0$ because the perturbation T' is small compared with T and T_0.

Equation (17) indicates that μ is a function of $\triangle S$, T_0, and the second order time derivatives of S and T evaluated at t^*.

For the nucleation events at $T_0 = 195\,\mathrm{K}$ shown in Fig. 7, our calculations indicate that $0.01 < \mu < 0.1\,\mathrm{s}^{-1}$. From Eq. (14) we deduce that the large range of N_i (10^{-3} to $10^6\,\mathrm{L}^{-1}$) obtained for these nucleation events must be due to a large range in J_max. If the differences in μ among the nucleation events can be ignored, at a chosen temperature N_i depends solely on J_max, which depends solely on $\triangle S$. In fact, setting $\mu = 0.05\,\mathrm{s}^{-1}$ and $T_0 = 195\,\mathrm{K}$ in Eqs. (14) and (16) we obtain a functional dependence of N_i on $\triangle S$ (the solid curve in Fig. 7a) that fits the numerical data well. The error that results from assuming constant μ is further discussed in Sect. 5.2.

For the special case of a temperature-limit event, the partial pressure of water vapor can be approximated as constant during the nucleation event for $t_0 < t < t_0 + \tau$, and so

$$\triangle S \approx -\frac{S_0 L_\mathrm{s}}{R_\mathrm{v} T_0^2} \triangle T, \tag{18}$$

where $\triangle T$ is the change in temperature during the nucleation event defined in Eq. (9), L_s is the latent heat of sublimation, and R_v is the gas constant of water vapour. With $\mu = 0.05\,\mathrm{s}^{-1}$ and $T_0 = 195\,\mathrm{K}$, from Eqs. (14)–(18) we obtain the solid curve in Fig. 7b that captures the dependence of N_i on $\triangle T$ as suggested by the simulations of temperature-limit events.

5.2 Sensitivity of INC to nucleation temperature and deposition coefficient

Using the formulae derived in Sect. 5.1 we can now explain the sensitivity of the numerical results to T_0 and the deposition coefficient α. The analytic functions of N_i-versus-$\triangle S$ and N_i-versus-$\triangle T$ vary with T_0 (because a_w^i depends on T_0, recall Eq. 16), but they are independent of the deposition coefficient α. As described further below, the analytic functions agree well with the numerical data for temperature-limit events but tend to overestimate INCs for vapour-limit events at larger T_0 and/or larger α.

For $\alpha = 0.1$, Fig. 8a shows that the analytic function of N_i-versus-$\triangle S$ is consistent with the numerical data, except for vapour-limit events at $T_0 = 210\,\mathrm{K}$ that produce more than $10^4\,\mathrm{L}^{-1}$ ice crystals. This error arises because μ has been assumed to be constant ($\mu = 0.05\,\mathrm{s}^{-1}$) and independent of $\triangle S$ in the calculation of the analytic curve. The error is larger for larger temperature.

For $\alpha = 1$, the analytic function of N_i-versus-$\triangle S$ also overestimates N_i for vapour-limit events (Fig. 9a). We again attribute this error to the assumption that μ is constant over the shown range of $\triangle S$. The deposition coefficient governs the growth rate of ice crystals and affects how the saturation ratio changes with time, and how μ changes with $\triangle S$ (a consequence of Eq. 17). Our calculation indicates that the rate of change of μ with respect to $\triangle S$ increases with α. For larger values of α, calculation of N_i (especially for vapour-limit events) must account for the variations in μ as $\triangle S$ varies.

For all values of T_0 and α tested here, the analytic function explains well the pattern of N_i-versus-$\triangle T$ for temperature-limit events (Figs. 8b and 9b). For vapour-limit events, Eq. (18) overestimates N_i (especially for large α) because it neglects the depletion of water vapour due to ice depositional growth.

5.3 Dependence of INC on the initial water vapour mixing ratio

The temperature time series $T(t)$ along the trajectory of an air parcel (recall Eq. 5) and the initial water vapour content r_0 of the parcel are two independent conditions to be specified for the simulations. The initial water vapour content r_0 has a one-to-one relationship with the temperature at the threshold of nucleation T_0 via Eq. (4). In Sect. 4 we have studied how the INC varies with the various forms of $T(t)$ for a *given* r_0 and a corresponding T_0. Here, on the other hand, we discuss how the INC varies as r_0 and T_0 vary for a *given* $T(t)$.

Now, consider air parcels with slightly different initial water vapour mixing ratios, r_0 and $r_0 + \delta r_0$. The nucleation temperatures for these air parcels are respectively T_0 and $T_0 + \delta T_0$ (see illustration in Figs. 3 and 10). For constant pressure, δr_0 and δT_0 are related by

$$\frac{\delta r_0}{r_0} = \frac{\delta e_\mathrm{sat}}{e_\mathrm{sat}} + \frac{1}{S_0}\frac{\mathrm{d}S_0}{\mathrm{d}T_0}\delta T_0 = \frac{L_\mathrm{s}}{R_\mathrm{v} T_0^2}\delta T_0 + \frac{1}{S_0}\frac{\mathrm{d}S_0}{\mathrm{d}T_0}\delta T_0 \tag{19}$$

by Eq. (4) and the Clausius–Clapeyron relation. The first term dominates the right hand side of Eq. (19), from which we obtain

$$\frac{\mathrm{d}T_0}{\mathrm{d}r_0} \approx \frac{R_\mathrm{v} T_0^2}{L_\mathrm{s} r_0}, \tag{20}$$

which indicates that T_0 increases monotonically with r_0. For a given temperature time series $T(t)$, the minimum temperature T_min experienced by the parcels is the same (see Fig. 10). It follows that $|\triangle T| = T_0 - T_\mathrm{min}$ increases monotonically with r_0. For temperature-limit events, N_i increases exponentially with $|\triangle T|$ (recall Fig. 7 and Eq. 18), and so it must increase exponentially with r_0. As r_0 increases, N_i increases until reaching a limit above which the nucleation event must be vapour-limit (see e.g. Fig. 7). Thus, for a given temperature time series, r_0 controls N_i and also determines whether the nucleation event is temperature- or vapour-limit.

For example, consider a temperature time series defined by a cooling rate associated with $w = +0.1\,\mathrm{m\,s}^{-1}$ between $t = 0$ and $t_\mathrm{s} = 5\,\mathrm{min}$, and a warming rate associated with $w = -0.1\,\mathrm{m\,s}^{-1}$ after t_s (see Fig. 10). This temperature time series is similar to the profiles we have studied earlier in Sect. 4.2. Consider three air parcels following this temperature time series, but for which $r_0 = \{1.78; 1.80; 1.82\} \times 10^{-5}\,\mathrm{kg\,kg}^{-1}$. All three air parcels experience nucleation, and in all cases $T_\mathrm{min} = 194.71\,\mathrm{K}$ occurs

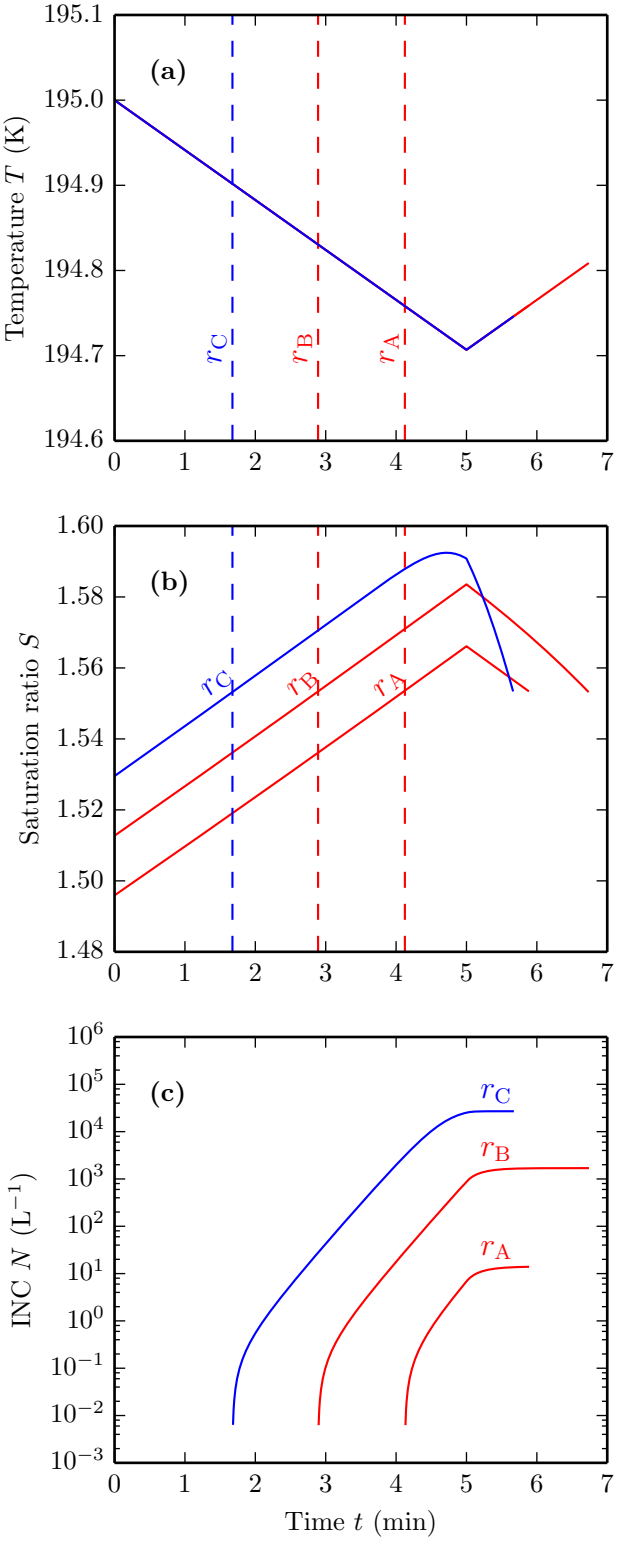

Figure 10. Evolution of temperature **(a)**, saturation ratio **(b)**, and INC **(c)** for three air parcels with slightly different initial water vapour mixing ratios: $\{r_A = 1.78;\ r_B = 1.80;\ r_C = 1.82\} \times 10^{-5}\,\mathrm{kg\,kg^{-1}}$. The parcels follow the same temperature time series as shown in **(a)**, but they begin nucleation at different times (indicated by the dash lines) and end up with widely different INCs.

during the nucleation periods. However, our calculations give $T_0 = \{194.76; 194.83; 194.90\}$ K and $N_i = \{1.4 \times 10^1; 1.7 \times 10^3; 2.7 \times 10^4\}\,\mathrm{L^{-1}}$ respectively for the three parcels. Moreover, the two drier air parcels experience temperature-limit nucleation events (red lines in Fig. 10), whereas the moist air parcel experiences a vapour-limit event (blue line in Fig. 10). As illustrated here, small differences in r_0 result in many orders of magnitude changes in N_i. Such a strong dependence of N_i on r_0 could explain the large-amplitude, small-scale heterogeneities in the INC as observed in cirrus clouds by Jensen et al. (2013).

6 Conclusions

We have simulated homogeneous ice nucleation using temperature time series data collected at high frequency by long-duration balloon flights near the tropical tropopause. The simulated nucleation events can be conceptually categorised as either vapour-limit or temperature-limit. For vapour-limit events, nucleation is limited by the depletion of water vapour. In contrast, for temperature-limit events, nucleation is controlled by the fluctuations in temperature (while the depletion in water vapour is negligible). The INC obtained for temperature-limit events is smaller than that obtained for vapour-limit events.

Our calculations of temperature-limit events confirm the finding by Spichtinger and Krämer (2013) that high-frequency fluctuations in temperature may limit the INC obtained by homogeneous freezing. Indeed, a small INC is obtained if the gravity waves produce large but non-persistent cooling rates such that the absolute drop in temperature (i.e. the difference between the temperature at the threshold of nucleation and the minimum temperature obtained during nucleation) remains small. This relationship between the INC and temperature has been illustrated here both empirically and analytically.

In addition to the fluctuations in temperature, small variations in the initial water vapour content of the air parcels can also lead to large variations in the INC obtained by nucleation. Moreover, post-nucleation processes acting during the cirrus life cycle contribute to modify the cloud original characteristics. Simulations of cirrus clouds in the TTL by Dinh et al. (2012, 2014) show that the INC decreases by several orders of magnitude as the cloud ages. For these reasons, we suggest that homogeneous ice nucleation (even acting alone in the absence of heterogeneous freezing) is not inconsistent with recent observations of cirrus clouds in the TTL, that indicate generally low but highly variable INC (Jensen et al., 2013).

Finally, it is encouraging that the INC for temperature-limit events does not depend on the deposition coefficient, a parameter still poorly constrained by theoretical understanding as well as laboratory measurements and field observations.

Acknowledgements. The data used for simulations in this work was collected during the project "Concordiasi," which is supported by the following agencies: Météo-France, CNES, CNRS/INSU, NSF, NCAR, University of Wyoming, Purdue University, University of Colorado, Alfred Wegener Institute, Met Office, and ECMWF. Concordiasi also benefited from the logistic and financial support of the Institut polaire français Paul Emile Victor (IPEV), Programma Nazionale di Ricerche in Antartide (PNRA), United States Antarctic Program (USAP), British Antarctic Survey (BAS), and from measurements by the Baseline Surface Radiation Network (BSRN) at Concordia.

Tra Dinh acknowledges support from the NOAA Climate and Global Change Postdoctoral Fellowship Program, and NSF grant AGS-1417659. This collaborative research emerged from Tra Dinh's visit to the Laboratoire de Météorologie Dynamique, which was supported by the "Tropical Cirrus" project of École Polytechnique's "Chaire pour le Développement Durable." Aurélien Podglajen, Albert Hertzog, Bernard Legras and Riwal Plougonven received support from the ANR project "Stradyvarius" (ANR-13-BS06-0011-01).

The authors would like to thank three anonymous reviewers, and Martina Krämer, Bernd Kärcher, and Daniel Knopf for helpful questions and comments that led to significant improvements of this work.

References

Barahona, D. and Nenes, A.: Parameterization of cirrus cloud formation in large-scale models: Homogeneous nucleation, J. Geophys. Res., 113, D11 211, doi:10.1029/2007JD009355, 2008.

Barahona, D. and Nenes, A.: Dynamical states of low temperature cirrus, Atmos. Chem. Phys., 11, 3757–3771, doi:10.5194/acp-11-3757-2011, 2011.

Boccara, G., Hertzog, A., Vincent, R. A., and Vial, F.: Estimation of gravity-wave momentum fluxes and phase speeds from quasi-Lagrangian stratospheric balloon flights. Part I: Theory and simulations, J. Atmos. Sci., 65, 3042–3055, doi:10.1175/2008JAS2709.1, 2008.

Brewer, A. W.: Evidence for a world circulation provided by the measurements of helium and water vapour distribution in the stratosphere, Q. J. Roy. Meteor. Soc., 75, 351–363, doi:10.1002/qj.49707532603, 1949.

Chen, Y., Kreidenweis, S. M., McInnes, L. M., Rogers, D. C., and DeMott, P. J.: Single particle analyses of ice nucleating aerosols in the upper troposphere and lower stratosphere, Geophys. Res. Lett., 25, 1391–1394, doi:10.1029/97GL03261, 1998.

Corti, T., Luo, B. P., Fu, Q., Vömel, H., and Peter, T.: The impact of cirrus clouds on tropical troposphere-to-stratosphere transport, Atmos. Chem. Phys., 6, 2539–2547, doi:10.5194/acp-6-2539-2006, 2006.

Davis, S., Hlavka, D., Jensen, E., Rosenlof, K., Yang, Q., Schmidt, S., Borrmann, S., Frey, W., Lawson, P., Voemel, H., and Bui, T. P.: In situ and lidar observations of tropopause subvisible cirrus clouds during TC4, J. Geophys. Res., 115, D00J17, doi:10.1029/2009JD013093, 2010.

Dinh, T. and Durran, D. R.: A hybrid bin scheme to solve the condensation/evaporation equation using a cubic distribution function, Atmos. Chem. Phys., 12, 1003–1011, doi:10.5194/acp-12-1003-2012, 2012.

Dinh, T. and Fueglistaler, S.: Cirrus, Transport, and Mixing in the Tropical Upper Troposphere, J. Atmos. Sci., 71, 1339–1352, doi:10.1175/JAS-D-13-0147.1, 2014a.

Dinh, T. and Fueglistaler, S.: Microphysical, radiative and dynamical impacts of thin cirrus clouds on humidity in the tropical tropopause layer and stratosphere, Geophys. Res. Lett., 41, 6949–6955, doi:10.1002/2014GL061289, 2014b.

Dinh, T., Durran, D. R., and Ackerman, T.: Cirrus and water vapor transport in the tropical tropopause layer – Part 1: A specific case modeling study, Atmos. Chem. Phys., 12, 9799–9815, doi:10.5194/acp-12-9799-2012, 2012.

Dinh, T., Fueglistaler, S., Durran, D., and Ackerman, T.: Cirrus and water vapour transport in the tropical tropopause layer – Part 2: Roles of ice nucleation and sedimentation, cloud dynamics, and moisture conditions, Atmos. Chem. Phys., 14, 12 225–12 236, doi:10.5194/acp-14-12225-2014, 2014.

Fueglistaler, S., Dessler, A. E., Dunkerton, T. J., Folkins, I., Fu, Q., and Mote, P. W.: Tropical tropopause layer, Rev. Geophys., 47, RG1004, doi:10.1029/2008RG000267, 2009.

Hermann, M., Zahn, A., Heinrich, G., and Brenninkmeijer, C. A. M.: Meridional distributions of aerosol particle number concentrations in the upper troposphere and lower stratosphere obtained by Civil Aircraft for Regular Investigation of the Atmosphere Based on an Instrument Container (CARIBIC) flights, J. Geophys. Res., 108, D3, doi:10.1029/2001JD001077, 2003.

Jensen, E. J., Toon, O. B., Pfister, L., and Selkirk, H. B.: Dehydration of the upper troposphere and lower stratosphere by subvisible cirrus clouds near the tropical tropopause, Geophys. Res. Lett., 23, 825–828, doi:10.1029/96GL00722, 1996.

Jensen, E. J., Pfister, L., Bui, T.-P., Lawson, P., and Baumgardner, D.: Ice nucleation and cloud microphysical properties in tropical tropopause layer cirrus, Atmos. Chem. Phys., 10, 1369–1384, doi:10.5194/acp-10-1369-2010, 2010.

Jensen, E. J., Pfister, L., and Bui, T. P.: Physical processes controlling ice concentrations in cold cirrus near the tropical tropopause, J. Geophys. Res., 117, D11 205, doi:10.1029/2011JD017319, 2012.

Jensen, E. J., Diskin, G., Lawson, R. P., Lance, S., Bui, T. P., Hlavka, D., McGill, M., Pfister, L., Toon, O. B., and Gao, R.: Ice nucleation and dehydration in the Tropical Tropopause Layer, Proc. Nat. Acad. Sci., 110, 2041–2046, doi:10.1073/pnas.1217104110, 2013.

Kärcher, B. and Lohmann, U.: A parameterization of cirrus cloud formation: Homogeneous freezing of supercooled aerosols, J. Geophys. Res., 107, D2, doi:10.1029/2001JD000470, 2002.

Kärcher, B., Dörnbrack, A., and Sölch, I.: Supersaturation Variability and Cirrus Ice Crystal Size Distributions, J. Atmos. Sci., 71, 2905–2926, doi:10.1175/JAS-D-13-0404.1, 2014.

Koop, T. and Zobrist, B.: Parameterizations for ice nucleation in biological and atmospheric systems., Physical chemistry chemical physics : PCCP, 11, 10 839–10 850, doi:10.1039/b914289d, 2009.

Koop, T., Luo, B., Tsias, A., and Peter, T.: Water activity as the determinant for homogeneous ice nucleation in aqueous solutions, Nature, 406, 611–614, doi:10.1038/35020537, 2000.

Krämer, M., Schiller, C., Afchine, A., Bauer, R., Gensch, I., Mangold, A., Schlicht, S., Spelten, N., Sitnikov, N., Borrmann, S., de Reus, M., and Spichtinger, P.: Ice supersaturations and cir-

rus cloud crystal numbers, Atmos. Chem. Phys., 9, 3505–3522, doi:10.5194/acp-9-3505-2009, 2009.

Lawson, R. P., Pilson, B., Baker, B., Mo, Q., Jensen, E., Pfister, L., and Bui, P.: Aircraft measurements of microphysical properties of subvisible cirrus in the tropical tropopause layer, Atmos. Chem. Phys., 8, 1609–1620, doi:10.5194/acp-8-1609-2008, 2008.

Lohmann, U. and Roeckner, E.: Influence of cirrus cloud radiative forcing on climate and climate sensitivity in a general circulation model, J. Geophys. Res., 100, 16 305, doi:10.1029/95JD01383, 1995.

Magee, N., Moyle, A. M., and Lamb, D.: Experimental determination of the deposition coefficient of small cirrus-like ice crystals near -50 Celsius, Geophys. Res. Lett., 33, L17 813, doi:10.1029/2006GL026665, 2006.

Massman, W. J.: On the nature of vertical oscillations of constant volume balloons, J. Appl. Meteor., 17, 1351–1356, doi:10.1175/1520-0450(1978)017<1351:OTNOVO>2.0.CO;2, 1978.

Murphy, D. M.: Rare temperature histories and cirrus ice number density in a parcel and one-dimensional model, Atmos. Chem. Phys. Discuss., 14, 10 701–10 723, doi:10.5194/acpd-14-10701-2014, 2014.

Murphy, D. M. and Koop, T.: Review of the vapour pressures of ice and supercooled water for atmospheric applications, Q. J. R. Meteorol. Soc., 131, 1539–1565, doi:10.1256/qj.04.94, 2005.

Nastrom, G. D.: The response of superpressure balloons to gravity waves, J. Appl. Meteor., 19, 1013–1019, doi:10.1175/1520-0450(1980)019<1013:TROSBT>2.0.CO;2, 1980.

Podglajen, A., Hertzog, A., Plougonven, R., and Žagar, N.: Assessment of the accuracy of (re)analyses in the equatorial lower stratosphere, J. Geophys. Res., 119, 11,166–11,188, doi:10.1002/2014JD021849, 2014.

Pruppacher, H. R. and Klett, J. D.: Microphysics of clouds and precipitation, D. Reidel Publishing Company, Dordrecht, Holland, 1978.

Rabier, F., Bouchard, A., Brun, E., Doerenbecher, A., Guedj, S., Guidard, V., Karbou, F., Peuch, V.-H., Amraoui, L. E., Puech, D., Genthon, C., Picard, G., Town, M., Hertzog, A., Vial, F., Cocquerez, P., Cohn, S. A., Hock, T., Fox, J., Cole, H., Parsons, D., Powers, J., Romberg, K., VanAndel, J., Deshler, T., Mercer, J., Haase, J. S., Avallone, L., Kalnajs, L., and Mechoso, C. R.: The Concordiasi project in Antarctica, Bull. Am. Meteorol. Soc., 91, 69–86, doi:10.1175/2009bams2764.1, 2010.

Ren, C. and Mackenzie, A. R.: Cirrus parametrization and the role of ice nuclei, Q. J. Roy. Meteor. Soc., 131, 1585–1605, doi:10.1256/qj.04.126, 2005.

Rogers, D. C., Demott, P. J., Kreidenweis, S. M., and Chen, Y.: Measurements of ice nucleating aerosols during SUCCESS, Geophys. Res. Lett., 25, 1383–1386, doi:10.1029/97GL03478, 1998.

Shi, X., Liu, X., and Zhang, K.: Effects of preexisting ice crystals on cirrus clouds and comparison between different ice nucleation parameterizations with the Community Atmosphere Model (CAM5), Atmos. Chem. Phys., 15, 1503–1520, doi:10.5194/acp-15-1503-2015, 2015.

Skrotzki, J., Connolly, P., Schnaiter, M., Saathoff, H., Möhler, O., Wagner, R., Niemand, M., Ebert, V., and Leisner, T.: The accommodation coefficient of water molecules on ice – cirrus cloud studies at the AIDA simulation chamber, Atmos. Chem. Phys., 13, 4451–4466, doi:10.5194/acp-13-4451-2013, 2013.

Spichtinger, P. and Krämer, M.: Tropical tropopause ice clouds: a dynamic approach to the mystery of low crystal numbers, Atmos. Chem. Phys., 13, 9801–9818, doi:10.5194/acp-13-9801-2013, 2013.

Vincent, R. A. and Hertzog, A.: The response of superpressure balloons to gravity wave motions, Atmos. Meas. Tech., 7, 1043–1055, doi:10.5194/amt-7-1043-2014, 2014.